1. INTRODUCTION AND EXPLANATORY NOTES[1]

Shipboard Scientific Party[2]

INTRODUCTION

The equatorial-subtropical Atlantic Ocean has from the outset figured prominently in the history of paleoceanography, beginning with the *Meteor* and Swedish Deep-Sea Expedition cruises, continuing with the oxygen isotopic work of Emiliani (1955), extending to the glacial climate reconstruction of CLIMAP (1981), and including rotary-drilling results from the Deep Sea Drilling Project (von Rad et al., 1982). The importance of this region can be attributed to several factors: excellent preservation of the calcareous fauna and flora, high sedimentation rates, wind-blown and fluvial delivery of diverse indicators of continental climate, and large bathymetric contrasts for studies of depth-dependent parameters.

Although several Deep Sea Drilling Project (DSDP) sites had been rotary-drilled in the subtropical Atlantic prior to Ocean Drilling Program (ODP) Leg 108, no hydraulic piston cores had been taken in this region for high-resolution paleoclimatic studies. The basic Leg 108 plan was to core Neogene sediments at 10 sites forming a north-south transect from 2°S to 23°N (Fig. 1).

This proposed transect spanned several major oceanic and atmospheric regimes (Sarnthein et al., 1982), each of which was a target of the proposed coring. Primary Neogene research objectives included determination of (1) the history of northern trade winds, monitored in cores along the coast of northwest Africa by oceanic indicators of nearshore oceanic upwelling intensity and productivity and by the composition and grain size of land-derived eolian dust; (2) the history of the northernmost annual advance of the Intertropical Convergence Zone (ITCZ), monitored by eolo-marine dust deposited during large outbreaks of the Saharan Air layer; (3) the history of southern trade winds, monitored in near-equatorial cores by diverse indicators of mid-ocean divergence and by dust tracer particles; and (4) past variations in bottom-water flow, particularly as shown by stable-isotopic indices of the degree of isolation of eastern Atlantic deep waters.

Other major Neogene objectives included (1) determining the history of cyclical North African aridity and monsoonal humidity, as indicated by eolian mineralogic and biogenic components in cores throughout the transect; (2) determining variations in the strength of bottom-water flow through Kane Gap, to be measured by erosional gaps correlated to prominent seismic reflectors and to stratigraphic gaps at other sites; (3) high-quality stable-isotopic records to monitor changes in global ice volume and low-latitude sea-surface temperature; and (4) a high-resolution paleomagnetic stratigraphy, with highly detailed studies of selected polarity transitions.

Additional objectives included (1) retrieval of dune-sand turbidites as indicators of continental aridity and downslope transport, (2) high-quality biostratigraphic studies of Neogene datums at low latitudes and in Eastern Boundary Current regimes, and (3) studies of carbonate dissolution and preservation in a time/depth framework.

From a broader perspective, the Leg 108 transect was designed to link up with six sites cored in the eastern North Atlantic from 37° to 54°N during DSDP Leg 94 (Ruddiman, Kidd, Thomas, et al., 1987) and three sites cored in the Norwegian Sea on ODP Leg 104 (Eldholm, Thiede, Taylor, et al., in press). Together, sites from these three legs represent a nearly continuous Neogene paleoenvironmental transect spanning the entire 70° latitude range of the eastern North Atlantic Ocean.

EXPLANATORY NOTES

Standard procedures for both drilling operations and preliminary shipboard analysis of the material recovered have been regularly amended and upgraded since 1968 during the Deep Sea Drilling Project and Ocean Drilling Program. In this chapter we have assembled information that will help the reader understand the basis for our preliminary conclusions and help the interested investigator select samples for further analysis. This information regards only shipboard operations and analyses described in the site reports in Part A or *Initial Report* of the Leg 108 *Proceedings of the Ocean Drilling Program*. Methods used by various investigators for further shore-based analysis of Leg 108 data will be detailed in the individual scientific contributions published in Part B or *Final Report* of the Leg 108 *Proceedings* volume.

Responsibility of Authorship

Authorship of the site reports is shared among the entire shipboard scientific party. The Leg 108 site chapters are organized into the following sections, with authors' names listed alphabetically in parentheses:

Site Summary (Ruddiman, Sarnthein)
Geologic Setting and Objectives (Ruddiman, Sarnthein)

[1] Ruddiman, W., Sarnthein, M., Baldauf, J., et al., 1988. *Proc., Init. Repts. (Pt. A), ODP*, 108.

[2] William Ruddiman (Co-Chief Scientist), Lamont-Doherty Geological Observatory, Palisades, NY 10964; Michael Sarnthein (Co-Chief Scientist), Geologisch-Paläontologisches Institut, Universität Kiel, Olshausenstrasse 40, D-2300 Kiel, Federal Republic of Germany; Jack Baldauf, ODP Staff Scientist, Ocean Drilling Program, Texas A&M University, College Station, TX 77843; Jan Backman, Department of Geology, University of Stockholm, S-106 91 Stockholm, Sweden; Jan Bloemendal, Graduate School of Oceanography, University of Rhode Island, Narragansett, RI 02882-1197; William Curry, Woods Hole Oceanographic Institution, Woods Hole, MA 02543; Paul Farrimond, School of Chemistry, University of Bristol, Cantocks Close, Bristol BS8 1TS, United Kingdom; Jean Claude Faugeres, Laboratoire de Géologie-Océanographie, Université de Bordeaux I, Avenue des Facultés Talence 33405, France; Thomas Janacek, Lamont-Doherty Geological Observatory, Palisades, NY 10964; Yuzo Katsura, Institute of Geosciences, University of Tsukuba, Ibaraki 305, Japan; Hélène Manivit, Laboratoire de Stratigraphie des Continents et Océans, (UA 319) Universitè Paris VI, 4 Place Jussieu, 75230 Paris Cedex, France; James Mazzullo, Department of Geology, Texas A&M University, College Station, TX 77843; Jürgen Mienert, Geologisch-Päläontologisches Institut, Universität Kiel, Olshausenstrasse 40, D-2300 Kiel, Federal Republic of Germany, and Woods Hole Oceanographic Institution, Woods Hole, MA 02543; Edward Pokras, Lamont-Doherty Geological Observatory, Palisades, NY 10964; Maureen Raymo, Lamont-Doherty Geological Observatory, Palisades, NY 10964; Peter Schultheiss, Institute of Oceanographic Sciences, Brook Road, Wormley, Godalming, Surrey GU8 5UG, United Kingdom; Rüdiger Stein, Geologisch-Päläontologisches Institut, Universität Giessen, Senckenbergstrasse 3, 6300 Giessen, Federal Republic of Germany; Lisa Tauxe, Scripps Institution of Oceanography, La Jolla CA 92093; Jean-Pierre Valet, Centre des Faibles Radioactivités, CNRS, Avenue de la Terrasse, 91190 Gif-sur-Yvette, France; Philip Weaver, Institute of Oceanographic Sciences, Brook Road, Wormley, Godalming, Surrey GU8 5UG, United Kingdom; Hisato Yasuda, Department of Geology, Kochi University, Kochi 780, Japan.

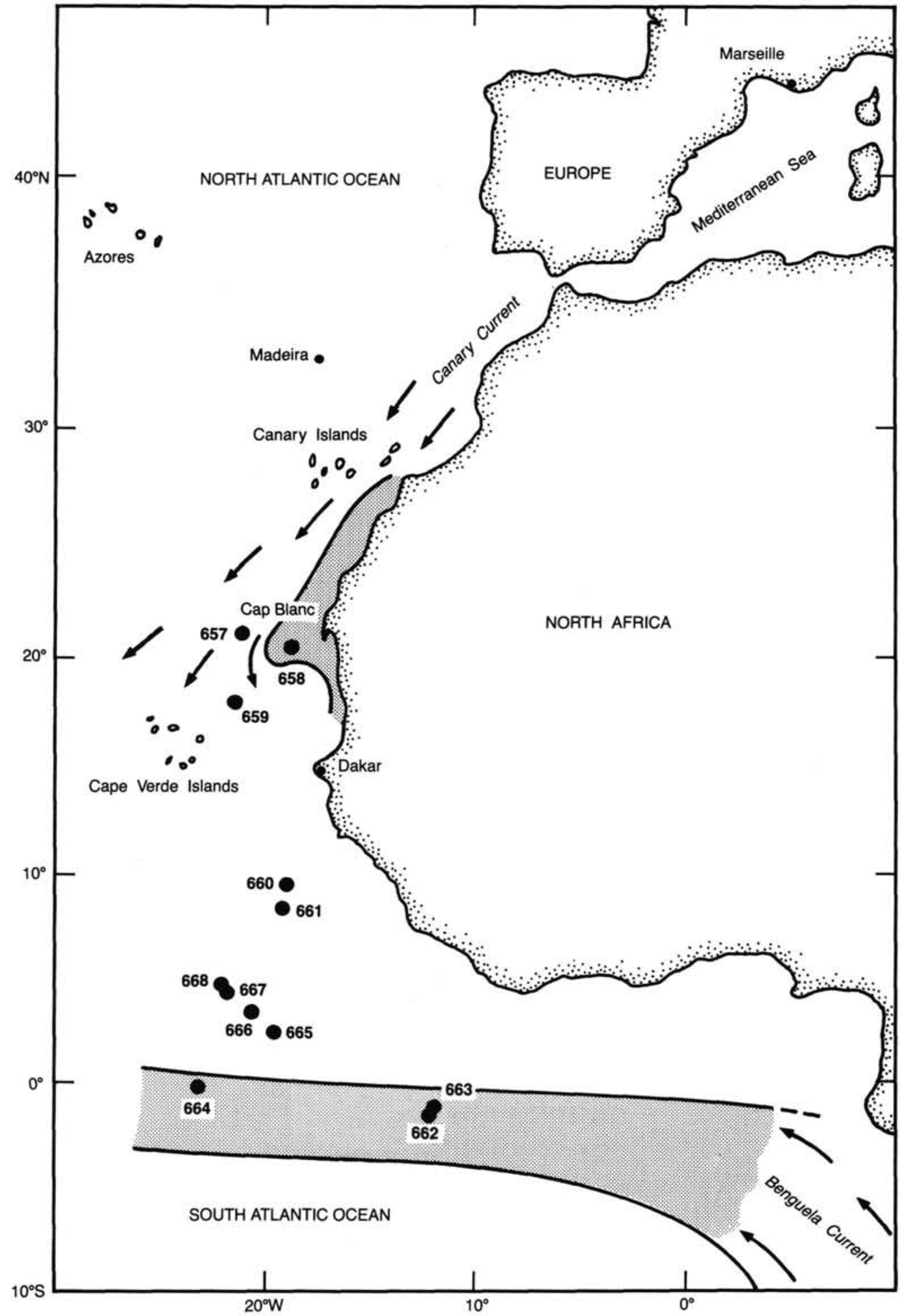

Figure 1. Location of sites cored during Leg 108. Arrows mark current systems; stippled areas indicate regions of strong Pliocene-Pleistocene upwelling and divergence.

Operations (Ruddiman, Sarnthein)
Lithostratigraphy and Sedimentology (Curry, Faugeres, Janecek, Katsura, Mazzullo, Stein)
Biostratigraphy (Backman, Baldauf, Manivit, Pokras, Raymo, Weaver, Yasuda)
Paleomagnetics (Bloemendal, Tauxe, Valet)
Accumulation Rates (Backman, Baldauf, Manivit, Pokras, Raymo, Tauxe, Valet, Weaver, Yasuda)
Organic Geochemistry (Farrimond, Stein)
Inorganic Geochemistry (Farrimond, Stein)
Physical Properties (Mienert, Schultheiss)
Logging (Ruddiman, Sarnthein)

Seismic Stratigraphy (Ruddiman, Sarnthein)
Composite Depth (Ruddiman, Sarnthein)
Appendix—Summary graphic lithologic and biostratigraphic logs, and core descriptions or "barrel sheets" (Shipboard Scientific Party)

Data and preliminary interpretations in the site chapters reflect knowledge gleaned only from shipboard and initial post-cruise analyses. Results of the more detailed shore-based work presented in the special-studies chapters in the second portion of this volume (Part B or *Final Report*) may in some cases necessitate reinterpretation of these preliminary site chapters.

Survey and Drilling Data

The survey data used for specific site selections are discussed in each site chapter. Short surveys using a precision echo sounder and seismic profiles were made on *JOIDES Resolution* approaching each site. All geophysical survey data collected during Leg 108 are presented in the "Underway Geophysics" chapter (this volume).

The seismic-profiling system consisted of two 80-in.^{3} water guns, one 400-in.^{3} water gun, one 300-in.^{3} air gun, a hydrophone array designed at Scripps Institution of Oceanography, Bolt amplifiers, two band-pass filters, and two EDO recorders, usually recording at two different filter settings.

Bathymetric data were displayed on 3.5- and 12-kHz Precision Depth Recorder systems, which consist of sound transceiver, transducer, and recorder. The depths were read on the basis of an assumed 1463 m/s sound velocity. The water depth (in meters) at each site was corrected (1) according to the tables of Matthews (1939) and (2) for the depth of the hull transducer (6.8 m) below sea level. In addition, depths referred to the drilling-platform level are assumed to be 10.5 m above the water line.

Drilling Characteristics

Because water circulation down the hole is open, cuttings are lost onto the seafloor and cannot be examined. The only available information about sedimentary stratification in uncored or unrecovered intervals, other than from seismic data or wireline-logging results, is from an examination of the behavior of the drill string as observed on the drill platform. The harder the layer being drilled, the slower and more difficult it usually is to penetrate. A number of other factors, however, determine the rate of penetration, so it is not always possible to relate this directly to the hardness of the layers. The parameters of bit weight and revolutions per minute are recorded on the drilling recorder and influence the rate of penetration.

Drilling Deformation

When cores are split, many show signs of significant sediment disturbance. Such disturbance includes the concave-downward appearance of originally horizontal bands, the haphazard mixing of lumps of different lithologies (mainly at the top of cores) and the near-fluid state of some sediments recovered from tens to hundreds of meters below the seafloor. Core deformation probably occurs during one of three different steps at which the core can suffer stresses sufficient to alter its physical characteristics: cutting, retrieval (with accompanying changes in pressure and temperature), and core handling on deck.

Shipboard Scientific Procedures

Numbering of Sites, Holes, Cores, and Samples

ODP drill sites are numbered consecutively from the first site drilled by *Glomar Challenger* in 1968. Site numbers are slightly different from hole numbers. A site number refers to one or more holes drilled while the ship is positioned over a single acoustic beacon. Several holes may be drilled at a single site by pulling the drill pipe above the seafloor (out of one hole), moving the ship some distance from the previous hole, and then drilling another hole.

For all ODP drill sites, a letter suffix distinguishes each hole drilled at the same site, for example: the first hole takes the site number with suffix *A*, the second hole takes the site number with suffix *B*, and so forth. This procedure is different from that used by the Deep Sea Drilling Project (Sites 1 through 624), but it prevents ambiguity between site- and hole-number designations.

The cored interval is measured in meters below the seafloor. The depth interval of an individual core is the depth below seafloor from where the coring operation began to the depth where the coring operation ended (Fig. 2). Each coring interval is generally up to 9.7 m long, which is the maximum length of a core barrel. The coring interval may, however, be shorter. "Cored intervals" are not necessarily adjacent to each other but may be separated by "drilled intervals." In soft sediment, the drill string can be "washed ahead" with the core barrel in place, but not recovering sediment, by pumping water down the pipe at high pressure to wash the sediment out of the way of the bit. If thin, hard rock layers are present, however, it is possible to get spotty sampling of these resistant layers within the washed interval.

Cores taken from a hole are numbered serially from the top of the hole downward. Maximum full recovery for a single core is 9.7 m of sediment or rock, which is in a plastic liner (6.6 cm ID), plus about a 0.2-m-long sample (without a plastic liner) in a core catcher. The core catcher is a device at the bottom of the core barrel that prevents the core from sliding out while the barrel is being retrieved from the hole. The sediment core, which is in the plastic liner, is then cut into 1.5-m-long sections that are numbered serially from the top of the sediment core (Fig. 3). When full recovery is obtained, the sections are numbered from 1 through 7, the last section being shorter than 1.5 m. The core-catcher sample is placed below the last section, labeled "Core Catcher" (CC), and is treated as a separate section.

When recovery is less than 100%, and if the sediment is contiguous, the recovered sediment is conventionally placed at the top of the cored interval, and then 1.5-m-long sections are numbered serially, starting with Section 1 at the top. There will be as many sections as needed to accommodate the length of the core recovered (Fig. 3): for example, 3 m of core sample in a plastic liner will be divided into two 1.5-m-long sections. Sections are cut starting at the top of the recovered sediment, and the last section can be shorter than the normal 1.5 m length. If, after the core has been split, fragments that are separated by a void appear to have been contiguous *in situ*, a note is made in the description of the section.

Samples are designated by distances in centimeters from the top of each section to the top and bottom of the sample interval in that section. A full identification number for a sample consists of the following information: (1) leg, (2) site, (3) hole, (4) core number and type, (5) section, and (6) interval in centimeters.

For example, the sample-identification number "108-661A-6H-3, 98–100 cm" means that a sample was taken between 98 and 100 cm from the top of Section 3 of hydraulic piston Core 6, from the first hole drilled at Site 661 during Leg 108. A sample from the core catcher of this core might be designated "108-661A-6H, CC, 8–9 cm."

All ODP core and sample identifiers include "core type." The following abbreviations are used: R = rotary barrel; H = hydraulic piston core (HPC); P = pressure core barrel; X = extended core barrel (XCB); B = drill-bit recovery; C = center-bit recovery; I = *in-situ* water sample; S = sidewall sample; W =

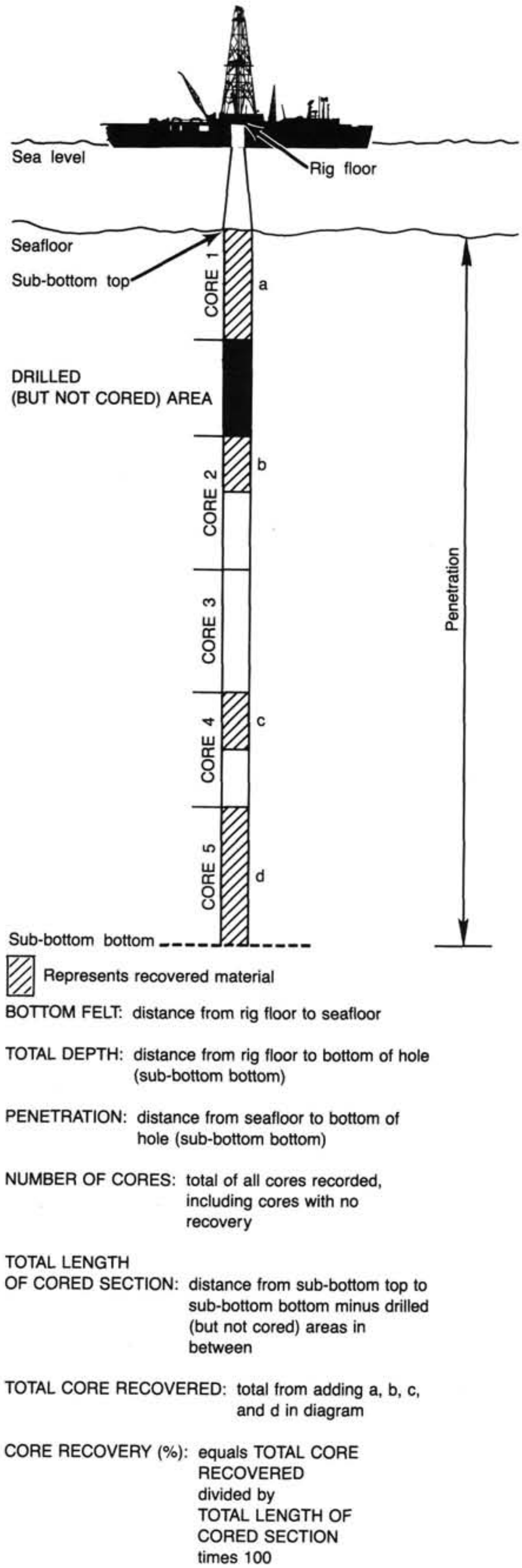

Figure 2. Diagram illustrating terms used in discussing coring operations and core recovery.

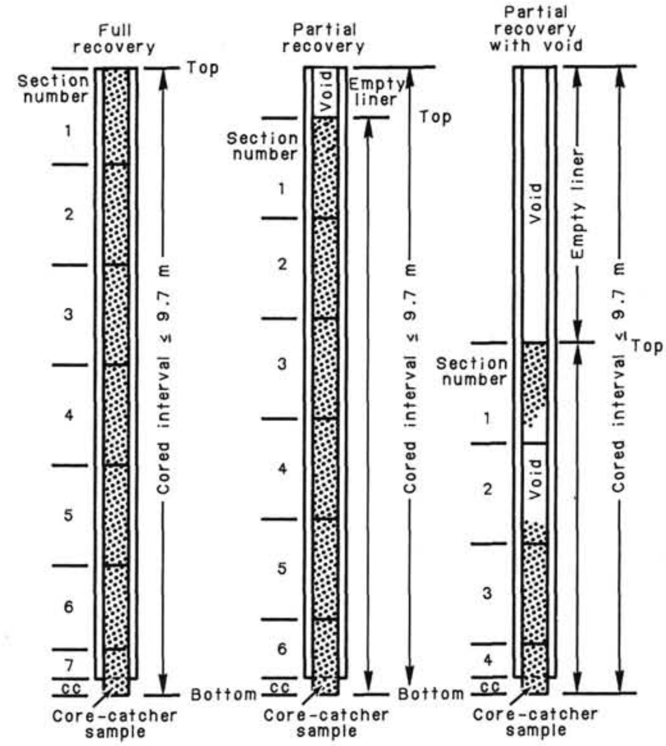

Figure 3. Diagram showing procedure in cutting and labeling of core sections.

wash core recovery; N = navidrill core; and M = miscellaneous material. Only HPC, XCB, and wash cores were drilled on ODP Leg 108.

The depth below the seafloor from which a sample numbered "108-661A-6H-3, 98–100 cm" was collected is the sum of the depth to the top of the cored interval for Core 6H (40.6 m) plus the 3 m included in Sections 1 and 2 (each 1.5 m long) plus the 98 cm below the top of Section 3. The sample in question is therefore from 44.58 meters below seafloor (mbsf). (Sample requests should refer to a specific interval within a core section rather than the depth below seafloor.)

Core Handling

During Leg 108, as soon as a core was retrieved on deck, a sample was taken from the core catcher and taken to the paleontology laboratory for an initial age assessment.

The core was then placed on the long horizontal rack, and gas samples were occasionally taken by piercing the core liner and withdrawing gas into a vacuum-tube sampler. Next, the core was marked into section lengths, each section was labeled, and the core cut into 1.5-m sections. Interstitial water (IW) and organic geochemistry (OG) whole-round samples were then taken. Each section was sealed at the top and bottom by gluing on a color-coded plastic cap, blue to identify the top of a section and clear for the bottom. A yellow cap was placed on section ends from which an IW whole-round sample had been taken. Red end caps were placed on section ends from which an OG sample had been taken. The caps were usually attached to the liner by coating the end of the liner and the inside rim of the end cap with acetone, and then the end caps were taped to the liner.

The cores were then carried into the laboratory, where the sections were again labeled using an engraver to mark the full designation of the section. The length of each section and the core-catcher sample was measured to the nearest centimeter, and this information was logged into the shipboard core-log database program.

The cores were then allowed to warm to room temperature (about 4 hr). After the cores had temperature-equilibrated, the whole-round sections were run through the Gamma Ray Attenuation Porosity Evaluation (GRAPE) device, the *P*-wave logger, the pass-through cryogenic magnetometer, and the magnetic-susceptibility device (see below). Thermal-conductivity measurements were occasionally also completed.

Cores of relatively soft material were split longitudinally into "working" and "archive" halves. The softer cores were split with a wire or saw, depending on the degree of induration. Harder cores were split with a band saw or diamond saw. As cores split with the wire on Leg 108 were split from top to bottom, younger material could possibly be transported downcore on the split face of each section. Scientists should be aware that the very near-surface part of the split core may be contaminated.

The working half of each core was sampled for both shipboard and shore-based laboratory studies. Each extracted sample was logged by the name of the investigator receiving the sample in the sample computer program. Records of all removed samples are kept by the Curator at ODP headquarters. The extracted samples were sealed in plastic vials or bags and labeled. Samples were routinely taken for shipboard analysis of sonic velocity by the Hamilton Frame method, water content by gravimetric analysis, percentage of calcium carbonate (carbonate bomb), and for other purposes. Many of these data are reported in the site chapters.

The color, texture, structure, physical disturbance by the drill bit, and composition of each archive half were described visually. Smear slides were made from samples taken from the archive half and were supplemented by thin sections taken from the working half. The archive half was then photographed with both black-and-white and color film, a whole core at a time.

Both halves were then put into labeled plastic tubes, sealed, and transferred to cold-storage space aboard the drilling vessel. Samples and whole-core sections collected for organic-geochemistry studies were frozen immediately on board ship and kept frozen. With the exception of eight frozen cores dedicated to geochemical analysis, Leg 108 cores are currently stored at the ODP East Coast Repository at Lamont-Doherty Geological Observatory, Palisades, New York. The dedicated geochemistry cores (Hole 658C) are stored at the ODP Gulf Coast Repository at Texas A&M University, College Station, Texas.

Core Description Forms ("Barrel Sheets")

The Core Description Forms (Fig. 4), or "barrel sheets," summarize the data obtained during the shipboard analysis of each core. The following discussion explains the ODP conventions used in compiling each part of the Core Description Forms and the exceptions to these procedures adopted by the Leg 108 scientists.

Core Designation

Cores are designated using leg, site, hole, and core number and type, as previously discussed. In addition, the cored interval is specified in terms of meters below sea level (mbsl) and meters below seafloor (mbsf). On Leg 108, these depths were based on the drill-pipe measurement, as reported by the SEDCO coring technician and the ODP operations superintendent.

Age Data

Microfossil abundances, preservation, and zone assignment, as determined by shipboard paleontologists, appear on the Core Description Form under the heading "Biostrat. Zone/Fossil Character." The geologic age determined from the paleontological results appears in the "Time-Rock" column. Detailed information on the zonations and terms used to report abundance and preservation appears below (see "Biostratigraphy" section, this chapter).

Paleomagnetic, Physical-Properties, and Chemical Data

Columns are provided on the Core Description Form to record paleomagnetic results, location of physical-properties samples, and chemical data. Additional information on shipboard procedures for collecting these types of data appears below (see "Magnetic Experiments," "Physical Properties," and "Organic Geochemistry" sections, this chapter). Total-organic-carbon values are marked *TOC* on the barrel sheets, whereas carbonate contents (calculated as weight percentages of $CaCO_3$) are marked *IC*.

Graphic-Lithology Column

The lithologic-classification scheme presented here is represented graphically on the Core Description Forms using the symbols illustrated in Figure 5. Modifications and additions made to the graphic-lithology representation scheme recommended by the JOIDES Sedimentary Petrology and Physical Properties Panel are discussed below (see "Sediment Classification" section, this chapter).

Sediment Disturbance

Recovered rocks, particularly soft sediments, may be slightly to extremely disturbed, and the condition of disturbance must be indicated on the Core Description Forms. The symbols for the six disturbance categories used for soft and firm sediments are shown in the "Drilling Disturbance" column in the Core Description Form (Fig. 4). The disturbance categories (Fig. 6) are defined as follows: (1) slightly disturbed: bedding contacts are slightly bent; (2) moderately disturbed: bedding contacts have undergone extreme bowing, and firm sediment is fractured; (3) highly disturbed: bedding is completely disturbed or homogenized by drilling, at some places showing symmetrical diapirlike structure; (4) soupy: water-saturated intervals have lost all aspects of original bedding; (5) biscuited: sediment is firm and broken into chunks 5 to 10 cm long; and (6) brecciated: indurated sediment is broken into angular fragments by the drilling process, perhaps along preexisting fractures.

Sedimentary Structures

The locations and types of sedimentary structures in a core are shown by graphic symbols in the "Sedimentary Structures" column in the Core Description Form (Fig. 4). Figure 6 gives the key for these symbols. It should be noted, however, that distinguishing between natural structures and structures created by the coring process may be extremely difficult.

Color

Colors of the sediment are determined by comparison with the Geological Society of America Rock-Color Chart (Munsell Soil Color Charts, 1971). Colors were determined immediately after the cores were split and while they were still wet.

Lithology

Lithologies are shown in the Core Description Form by one or more of the symbols shown in Figure 5. The symbols in a group, such as CB1 or SB5, correspond to end-members of sediment compositional range, such as nannofossil ooze or radiolarite. For sediments that are mixtures of siliciclastic and biogenic sediments, the symbol for the siliciclastic constituents is on the left side of the column, the symbol for the biogenic constituents is on the right side of the column, and the abundances of the constituents approximately equal the percentage of the width of the graphic column that its symbol occupies. For example, the left 20% of the column may have a diatom ooze symbol (SB1), whereas the right 80% may have a clay symbol (T1), indicating sediment composed of 80% clay and 20% diatoms. Within this column, solid vertical lines are used to refer to

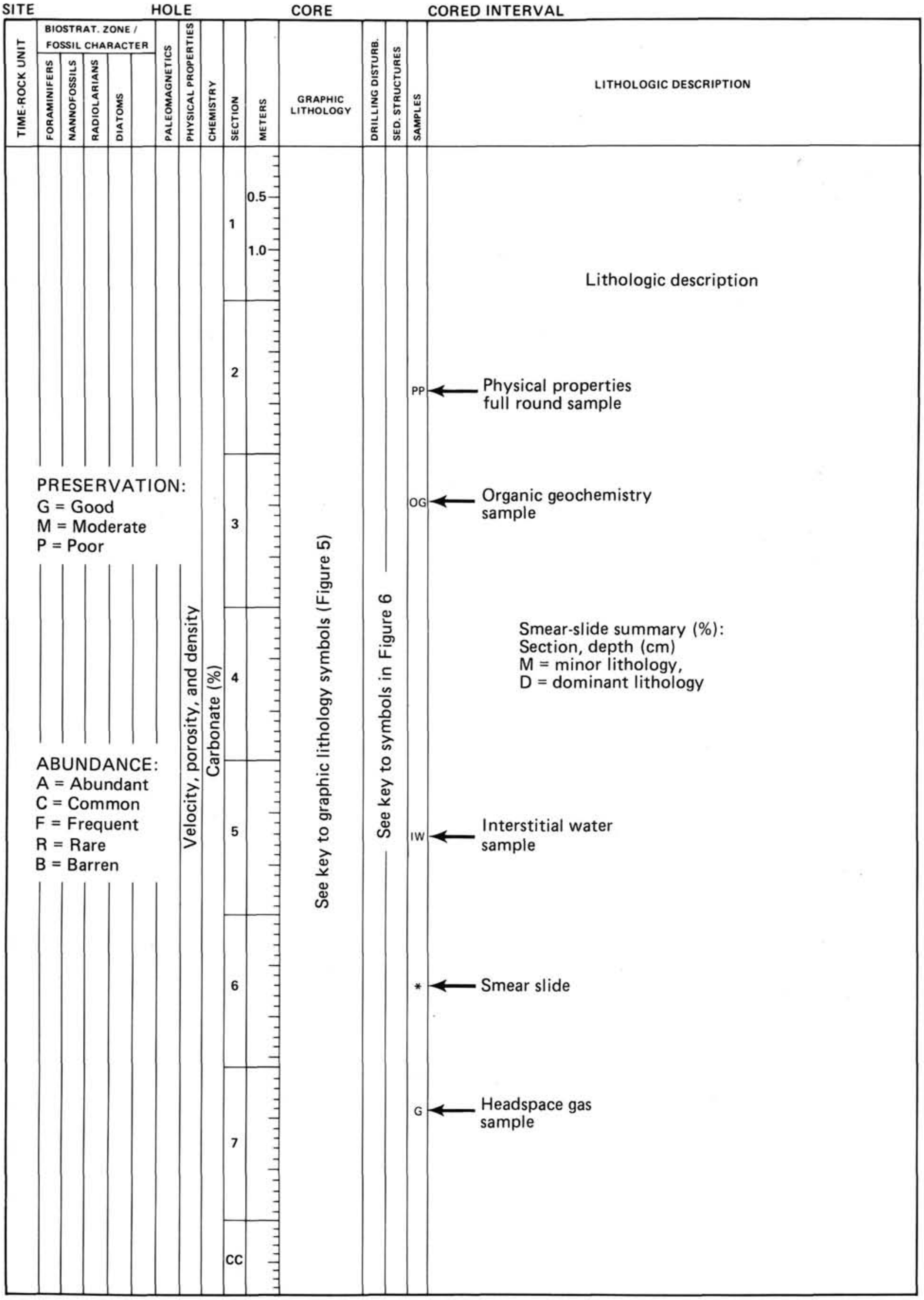

Figure 4. Core Description Forms ("barrel sheets") used for sediments and sedimentary rocks.

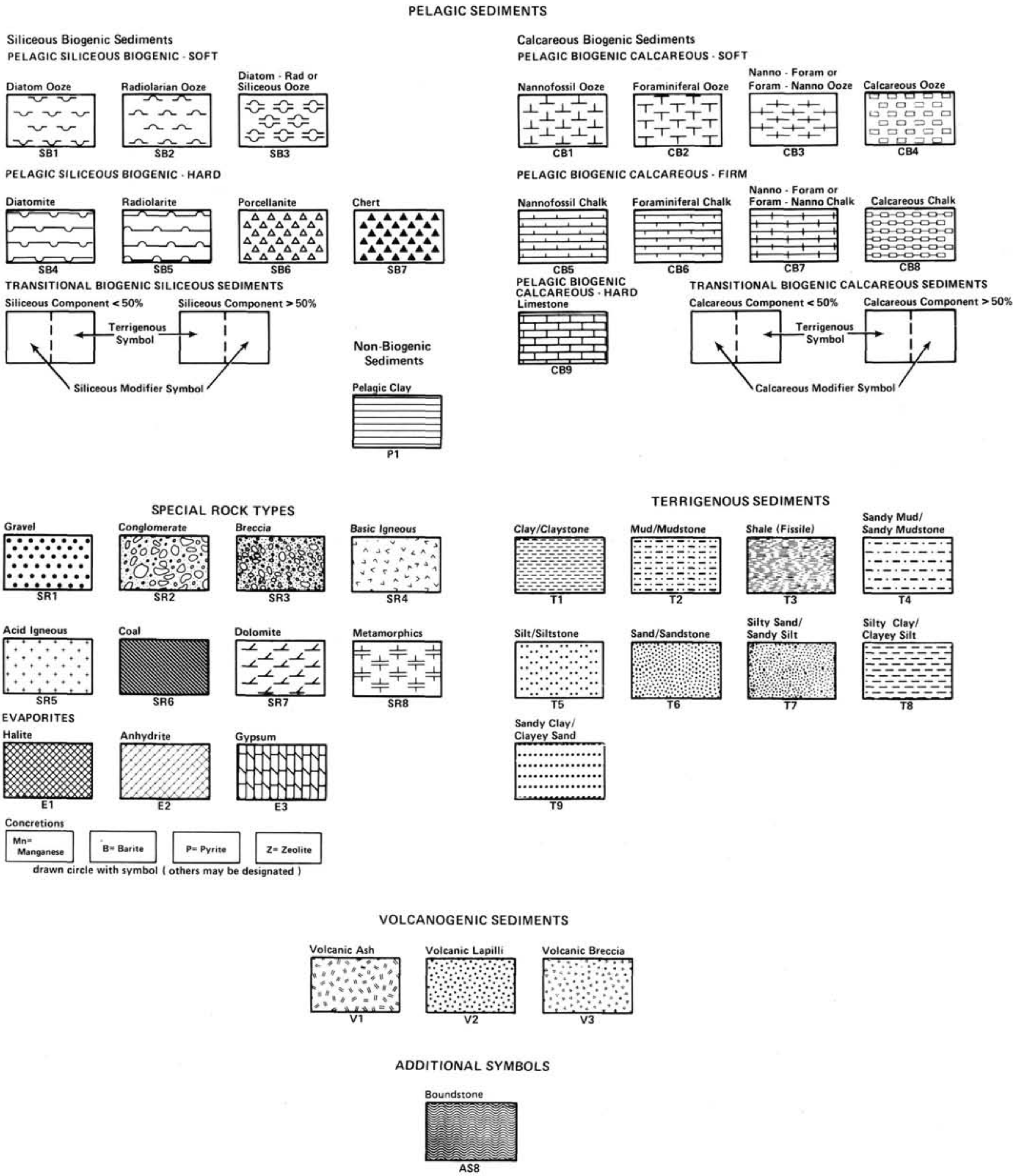

Figure 5. Graphic symbols to accompany the lithologic-classification scheme. Symbols are used in the "Graphic Lithology" column on the Core Description Form (see Fig. 4).

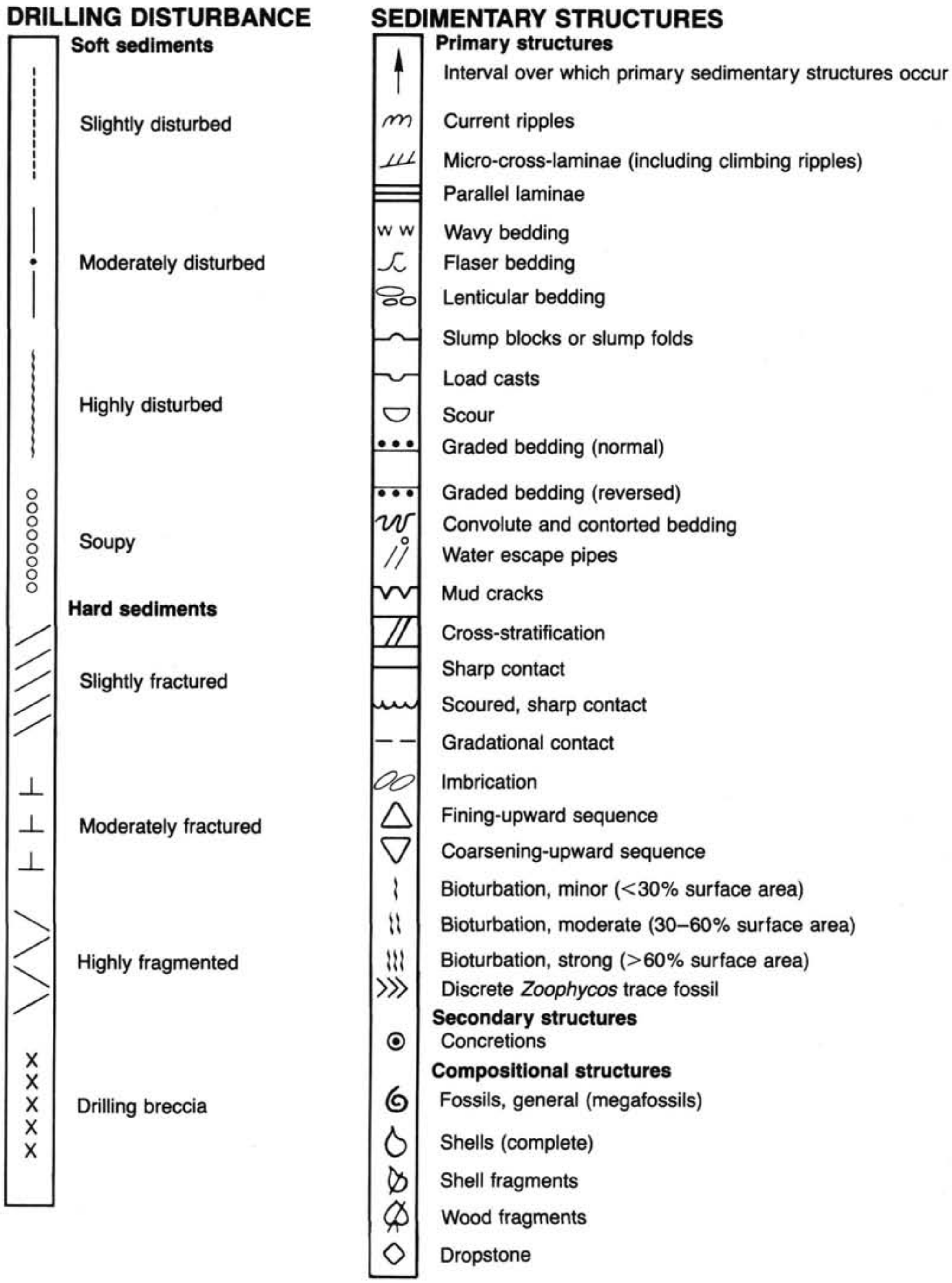

Figure 6. Symbols showing drilling disturbance and sedimentary structures used on the Core Description Form (see Fig. 4).

alternating sequences, while dashed vertical lines are used to refer to the major components in the particular sediment type.

Samples

The positions of samples taken from each core for shipboard analysis are indicated in the "Samples" column in the Core Description Form. An asterisk indicates the location of a smear slide sample. The symbols *IW*, *OG*, and *PP* designate whole-round intersitial water, frozen organic geochemistry, and physical-properties samples, respectively.

Although not indicated in the "Samples" column, the positions of samples for routine carbonate-bomb analyses are indicated by a circle in the "Chemistry" column. The positions of routine and additional physical-properties samples are recorded in Schultheiss and Mienert (this volume).

Shipboard paleontologists usually base their age determinations on core-catcher samples, although additional samples from other parts of the core may be examined when required.

Lithologic Description—Text

The lithologic description that appears on each Core Description Form consists of two parts: (1) a brief summary of the major lithologies observed in a given core in order of importance followed by a description of sedimentary structures of features, and (2) a description of minor lithologies observed in the core, including data on color, occurrence in the core, and significant features.

Smear Slide Summary

A table summarizing smear-slide and thin-section data, if available, appears on each Core Description Form. The section and interval from which the sample was taken are noted as well as identification as a dominant (*D*) or minor (*M*) lithology in the core. The percentage of all identified components (totaling 100%) is listed. As explained below, these data are used to classify the recovered material.

Sediment Classification

Lithologic Classification of Sediments

The sediment-classification scheme that is used on Leg 108 is a modified version of the sediment-classification system that was devised by the JOIDES Sedimentary Petrology and Physical Properties Panel (SP4) and adopted for use by the JOIDES Planning Committee in March 1974. The classification scheme used on Leg 108 incorporates many of the suggestions and terminologies of Dean et al. (1985). This classification scheme is descriptive rather than generic in nature—that is, the basic sediment types are defined on the basis of their texture and composition rather than on the basis of their assumed origin. The texture and composition of sediment samples, and the areal abundances of grain-components, were commonly estimated by the examination of smear slides with a petrographic microscope and thus may differ from more accurate measurements of texture and composition. The composition of some sediment samples was determined by more accurate methods, however, such as by coulometer and X-ray-diffraction analyses, in the shipboard laboratories.

This sediment-classification scheme differs from the conventional JOIDES sediment-classification scheme in one major way: the boundary between siliciclastic and biogenic sediments has been shifted from 30% to 50% (Fig. 7). This modification was made because one major objective of Leg 108 was to monitor the influx of siliciclastic grains from northwest Africa, but the JOIDES sediment-classification scheme does not accurately represent the relative proportions of siliciclastic grains that are present in samples that are mixtures of siliciclastic and biogenic grains. For example, if a sample contains 35% calcareous biogenic grains (e.g., nannofossils) and 65% siliciclastic grains (e.g., silt), the JOIDES sediment-classification scheme would classify it as a "marly nannofossil ooze or chalk"—clearly an inaccurate description of the composition of the sample. Our modification of the JOIDES sediment-classification scheme, on the other hand, would classify the samples on the basis of the composition of the majority of the grains within them. In the latter example, our sediment-classification scheme would classify this sample as a "nannofossil silt," which is a more accurate description of its composition.

General Rules of Classification

Every sample of sediment is assigned a main name that defines its sediment type, a major modifier(s) that describes the compositions and/or textures of grains that are present in abundance between 25% and 100%, and a minor modifier(s) that describes the compositions and/or textures of grains that are present in abundances between 10% and 25%. Grains that are present in abundances between 0% and 10% are considered insignificant and are not included in this classification.

The minor modifiers are always listed first in the string of terms that describes a sample and are attached to the suffix "-bearing," which distinguishes them from major modifiers. When two or more minor modifiers are employed, they are listed in order of increasing abundance. The major modifiers are always listed second in the string of terms that describes a sample and are also listed in order of increasing abundance. The main name is the last term in the string.

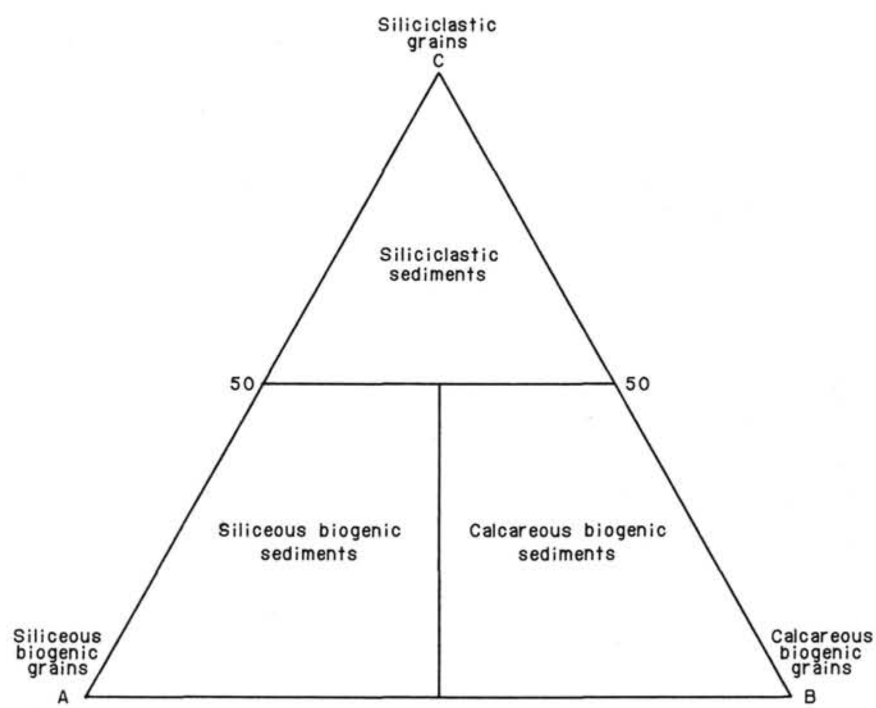

Figure 7. Ternary diagram that defines the three basic sediment types on the basis of the relative proportions of siliciclastic, siliceous biogenic, and calcareous biogenic grains.

The types of main names and modifiers that are employed in this classification scheme differ among the three basic sediment types (Table 1) and are described in succeeding sections.

Basic Sediment Types: Definitions

Three basic sediment types are defined on the basis of variations in the relative proportions of siliciclastic, siliceous biogenic, and calcareous biogenic grains: siliciclastic sediments, siliceous biogenic sediments, and calcareous biogenic sediments (Table 1 and Fig. 7).

Siliciclastic Sediments

Siliciclastic sediments are composed of greater than 50% terrigenous and volcaniclastic grains (i.e., rock and mineral fragments) and less than 50% calcareous and siliceous biogenic grains.

The main name for a siliciclastic sediment describes the textures of the siliciclastic grains and its degree of consolidation. The Wentworth (1922) grain-size scale (Table 2) is used to define the textural-class names for siliciclastic sediments that contain greater amounts of terrigenous grains than volcaniclastic grains. A single textural-class name (e.g., "sand," "coarse silt") is used when one textural class is present in abundances greater than 90%. When two or more textural classes are present in abundances greater than 10%, they are listed in order of increasing abundance (e.g., "silty sand," "ashy clay"). The term *mud* is used to describe mixtures of silt and clay.

The major and minor modifiers for a siliciclastic sediment describe the compositions of the siliciclastic grains as well as the compositions of accessory biogenic grains. The compositions of terrigenous grains can be described by terms such as "quartz," "feldspar," "glauconite," or "lithic" (for rock-fragments), and the compositions of volcaniclastic grains can be described by the terms "vitric" (glass), "crystalline," or "lithic." All compositional modifiers are followed by the suffix "-bearing" when the grain-component is present in minor (10%–25%) amounts. The compositions of biogenic grains can be described by terms that are given below.

Table 1. Summary of nomenclature of basic sediment types.

Minor modifiers	Major modifiers	Main name
	Siliciclastic sediments	
1. Composition of minor siliciclastic grains	1. Composition of major siliciclastic grains	1. Texture of terrigenous grains (sand, silt, etc.)
2. Composition of minor biogenic grains	2. Composition of minor biogenic grains	2. Texture of volcaniclastic grains (ash, lapilli, etc.)
	Siliceous biogenic sediments	
Minor modifiers	Major modifiers	Main name
1. Composition of minor biogenic grains	1. Composition of major biogenic grains	1. Ooze 2. Radiolarite 3. Diatomite 4. Porcellanite 5. Chert
2. Texture of minor siliciclastic grains	2. Texture of major siliciclastic grains	
	Calcareous biogenic sediments	
Minor modifiers	Major modifiers	Main name
1. Composition of minor biogenic grains	1. Composition of major biogenic grains	1. Ooze 2. Chalk 3. Limestone
2. Composition of minor siliciclastic grains	2. Composition of major siliciclastic grains	

Siliceous Biogenic Sediments

Siliceous biogenic sediments are composed of less than 50% siliciclastic grains and greater than 50% biogenic grains, but they contain greater proportions of siliceous biogenic grains than calcareous biogenic grains.

The main name of a siliceous biogenic sediment describes its degree of consolidation and/or its composition, using the terms (1) *ooze*: soft, unconsolidated siliceous biogenic sediment; (2) *radiolarite*: hard, consolidated siliceous biogenic sediment composed predominantly of radiolarians; (3) *diatomite*: hard, consolidated siliceous biogenic sediment composed predominantly of diatoms; (4) *porcellanite*: dull, white, porous indurated siliceous biogenic sediment; and (5) *chert*: lustrous, conchoidally fractured, indurated siliceous biogenic sediment.

The major and minor modifiers for a siliceous biogenic sediment describe the compositions of the siliceous biogenic grains as well as the compositions of accessory calcareous biogenic grains and the textures of accessory siliciclastic grains. The compositions of siliceous biogenic grains can be described by the terms "radiolarian," "diatom," "spicular," and "siliceous" (for unidentifable siliceous biogenic debris), followed by the suffix

Table 2. Grain-size scale (Wentworth, 1922) for terrigenous grains.

	Millimeters	Microns	Phi (ϕ)	Wentworth size class
			−0.20	
	4096		−0.12	
	1024		−0.10	Boulder (−0.8 to −0.12 ϕ)
	256		−0.8	Cobble (−0.6 to −0.8 ϕ)
	64		−0.6	
	16		−4	Pebble (−0.2 to −0.6 ϕ)
	4		−2	
	3.36		−1.75	
	2.83		−1.5	Granule
	2.38		−1.25	
	2.00		−1.0	
	1.68		−0.75	
	1.41		−0.5	Very coarse sand
	1.19		−0.25	
	1.00		0.0	
	0.84		0.25	
	0.71		0.5	Coarse sand
	0.59		0.75	
1/2	0.50	500	1.0	
	0.42	420	1.25	
	0.35	350	1.5	Medium sand
	0.30	300	1.75	
1/4	0.25	250	2.0	
	0.210	210	2.25	
	0.177	177	2.5	Fine sand
	0.149	149	2.75	
1/8	0.125	125	3.0	
	0.105	105	3.25	
	0.088	88	3.5	Very fine sand
	0.074	74	3.75	
1/16	0.0625	63	4.0	
	0.053	53	4.25	
	0.044	44	4.5	Coarse silt
	0.037	37	4.75	
1/32	0.031	31	5.0	
1/64	0.0156	15.6	6.0	Medium silt
1/128	0.0078	7.8	7.0	Fine silt Very fine silt
1/256	0.0039	3.9	8.0	
	0.0020	2.0	9.0	
	0.00098	0.98	10.0	
	0.00049	0.49	11.0	Clay
	0.00024	0.24	12.0	
	0.00012	0.12	13.0	
	0.00006	0.06	14.0	

"-bearing" when the component is present in minor (10%-25%) amounts. The compositions of accessory calcareous grains are described by terms that are discussed below; the textures of accessory terrigenous grains are described by terms that are discussed in the previous section.

Calcareous Biogenic Sediments

Calcareous biogenic sediments are composed of less than 50% siliciclastic grains and greater than 50% biogenic grains, but they contain greater proportions of calcareous biogenic grains than siliceous biogenic grains.

The main name of a calcareous biogenic sediment describes its degree of consolidation, using the terms *ooze* (soft, unconsolidated), *chalk* (partially to firmly consolidated), and *limestone* (hard, consolidated).

The major and minor modifiers for a calcareous biogenic sediment describe the compositions of calcareous biogenic grains as well as the compositions of accessory siliceous biogenic grains and the textures of accessory siliciclastic grains.

The compositions of calcareous biogenic grains are described by the terms *foraminifer, nannofossil*, or *calcareous* (for unidentifiable carbonate fragments), followed by the suffix "-bearing" when the grain-components are present in minor (10%-25%) amounts. The compositions of siliceous biogenic grains and the textures of siliciclastic grains are described by the terms discussed above.

Special Rock Types

The definitions and nomenclatures of special rock types are not included in the previous section but will adhere as closely as possible to conventional terminology. Rock types that are included in this category include authigenic minerals (e.g., pyrite, manganese, and zeolite), evaporites (e.g., halite and anhydrite), shallow-water limestones (e.g., carbonate grainstones and packstones), and extrusive igneous rocks (e.g., basalt).

Magnetostratigraphy

Time scales are syntheses of three independently varying aspects: correlation, calibration, and terminology. We have chosen the time scale of Berggren et al. (1985a, 1985b, 1985c) as our working model, as it is the most complete synthesis available. There is a discrepancy within Berggren et al. (1985a) as to the age assigned to the early/late Oligocene boundary. Berggren et al. (1985a, Fig. 5) indicate an age of 30.0 Ma, while in the text (Berggren et al., 1985a, Table 3) an age of 30.6 Ma is indicated. We adhere to an age of 30.0 Ma for the early/late Oligocene boundary. Table 3 shows the assigned age for the normal polarity intervals for the Oligocene through Pleistocene.

Correlations of the major fossil groups to the magnetic polarity time scale are shown in Figure 8 (Pliocene and Pleistocene), Figure 9 (Miocene) and Figure 10 (Oligocene). We hope that the sediments recovered during Leg 108 will provide confirmation of or refinements to this aspect of the time scale.

The calibration of the Berggren et al. (1985a) time scale is based on an interpretation of many radiometric dates tied into the magnetic-polarity pattern and, as such, provides reasonable estimates of absolute ages of biostratigraphic events. The accuracy of the dates is probably about 10% (Tauxe et al., 1985), whereas the precision of correlation is much better.

The terminology of the magnetic time scale has experienced dramatic changes and is still in a state of flux. The first magnetic time scale, derived from a worldwide distribution of basalts, was divided into "epochs" (Cox et al., 1963), later named Brunhes, Matuyama, and Gauss (Cox et al., 1964). Hays and Opdyke (1967) extended the epoch system, defining new time units based on the magnetostratigraphy of deep-sea sediments.

Table 3. Geomagnetic polarity time scale for Oligocene through Pleistocene time.

Normal polarity interval (Ma)	Anomaly	Normal polarity interval (Ma)	Anomaly
0-0.73	1	14.87-14.96	5B
0.91-0.98		15.13-15.27	5B
1.66-1.88	2	16.22-16.52	5C
2.02-2.04		16.56-16.73	5C
2.12-2.14		16.80-16.98	5C
2.47-2.92	2A	17.57-17.90	5D
2.99-3.08	2A	18.12-18.14	5D
3.18-3.40	2A	18.56-19.09	5E
3.88-3.97	3	19.35-20.45	6
4.10-4.24	3	20.88-21.16	6A
4.40-4.47	3	21.38-21.71	6A
4.57-4.77	3	21.90-22.06	
5.35-5.53	3A	22.25-22.35	
5.68-5.89	3A	22.57-22.97	6B
6.37-6.50		23.27-23.44	6C
6.70-6.78	4	23.55-23.79	6C
6.85-7.28	4	24.04-24.21	6C
7.35-7.41	4	25.50-25.60	7
7.90-8.21	4A	25.67-25.97	7
8.41-8.50	4A	26.38-26.56	7A
8.71-8.80		26.86-26.93	8
8.92-10.42	5	27.01-27.74	8
10.54-10.59		28.15-28.74	9
11.03-11.09		28.80-29.21	9
11.55-11.73	5A	29.73-30.03	10
11.86-12.12	5A	30.09-30.33	10
12.46-12.49		31.23-31.58	11
12.58-12.62		31.64-32.06	11
12.83-13.01		32.46-32.90	12
13.20-13.46		35.29-35.47	13
13.69-14.08		35.54-35.87	13
14.20-14.66			

The epochs were correlated to the magnetic anomaly pattern, first used by Vine and Matthews (1963) as key evidence for the process of seafloor spreading and then by later workers (e.g., Hays and Opdyke, 1967; Ryan et al., 1974). Because the term *epoch* has a previously defined connotation in stratigraphy, a subcommission on stratigraphic nomenclature recommended that magnetic epochs be referred to as *chrons* (Hedberg et al., 1979).

Unfortunately, the long-accepted correlation of Chron 9 to Anomaly 5 (the Rosetta Stone of the Neogene time scale), proposed initially by Ryan et al. (1974), is now considered to be in error (Miller et al., 1985; Berggren et al., 1985a). The preferred correlation is now Chron 11 to Anomaly 5. Thus the literature faces a grave danger of ambiguity when using Miocene chron names. Following LaBrecque et al. (1983), who proposed an anomaly-based chron terminology for the Paleogene, Berggren et al. (1985a, 1985b, 1985c) recommend the adoption of the chron structure proposed by Cox (1982) but with the addition of a prefix letter *C* (for correlative). Although in their Figure 6 (Neogene time scale) they use the "new-old" terminology, we will use that recommended in the text as shown in our Figures 8 through 10. By adopting an entirely new, anomaly-based chron system, we hope to escape from the labyrinth of magnetostratigraphic terminology. Throughout the site chapters of this volume, we will indicate a specific point in time as *Ma* (for example, 5 Ma = 5 million years ago) and an interval of time as m.y. (for example, a duration of 5 m.y. between 5 and 10 Ma).

Biostratigraphy

Calcareous Nannofossils

The two best-known zonal schemes for Cenozoic calcareous nannofossils are those of Martini (1971) and Bukry (1973, 1975). Martini (1971) introduced a code system whereby Zone NN1

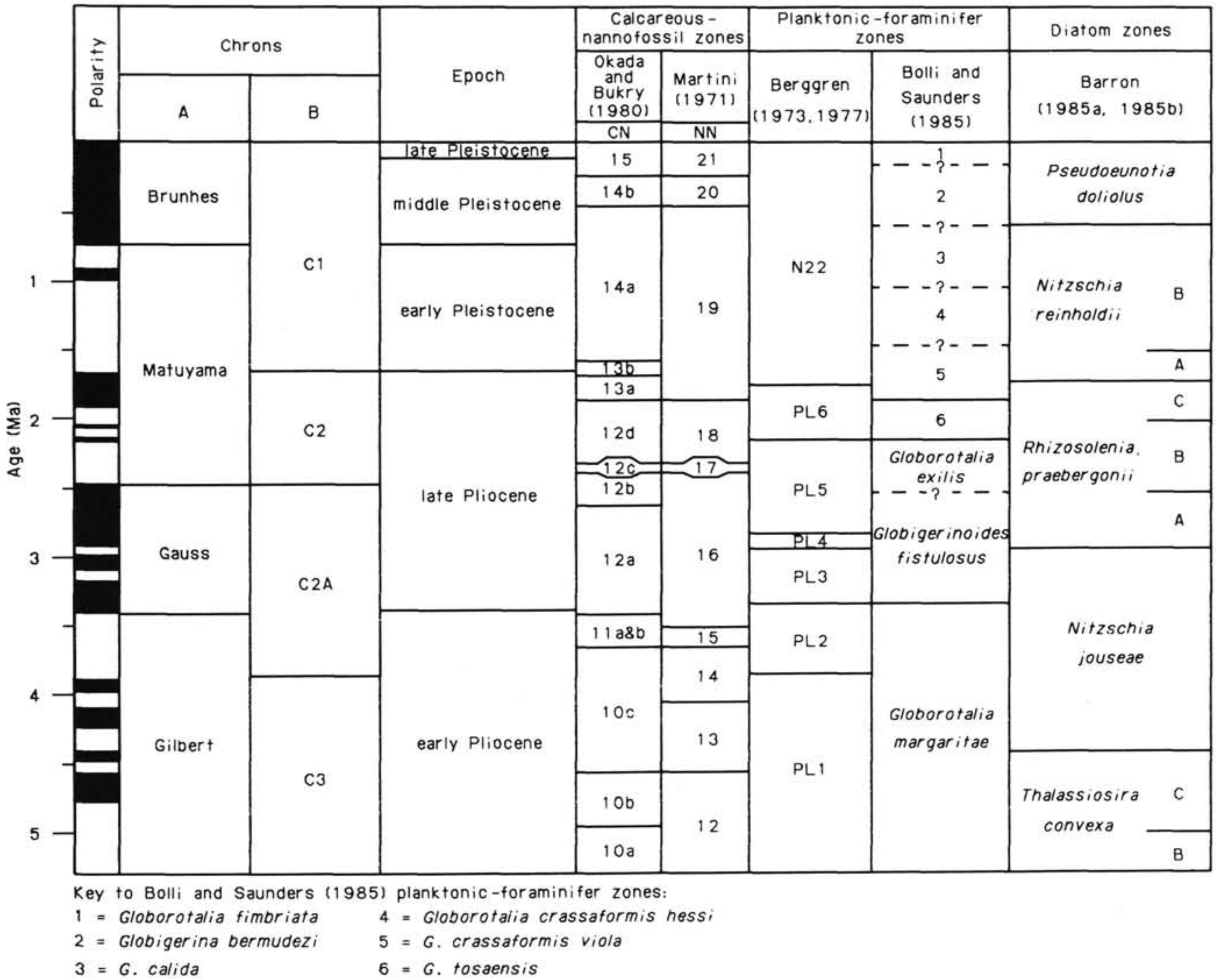

Figure 8. Pliocene and Pleistocene geochronology of Berggren et al. (1985a, 1985b) used during Leg 108.

through Zone NN21 represents the Neogene and Zone NP1 through Zone NP25 represents the Paleogene, from oldest to youngest. Martini (1971) based his zonal scheme on studies of material representing both mid- and low-latitude areas, whereas Bukry's (1973, 1975) zonal scheme reflects material collected entirely from low-latitude areas.

Okada and Bukry (1980) subsequently introduced code numbers to Bukry's (1973, 1975) biostratigraphic zones (and subzones). The 19 CP zones (and 20 subzones) represent the Paleogene, and the 15 CN zones (and 24 subzones) represent the Neogene. In analogy with Martini's scheme, Okada and Bukry (1980) gave the lowest code number (zone 1) to the oldest stratigraphic unit and vice versa. For example, Zone CN11 is older than Zone CN12, and Subzone CN12a is older than Subzone CN12b. It is noteworthy that Bukry (1985) changed the name of Subzone CN12d from the *Calcidiscus macintyrei* Subzone to the *Discoaster triradiatus* Subzone in order "to avoid duplication of names with the *Calcidiscus macintyrei* Zone of Gartner (1977)."

The zonal schemes of Martini (1971) and Okada and Bukry (1980) show many similarities because, by and large, they use the same species events (first/last occurrences) to define their zonal (or subzonal) boundaries. All latest Eocene through Pleistocene marker species used in the zonal schemes mentioned above are listed in Table 4, together with their assigned age estimates.

Some auxiliary biostratigraphic markers that are not included in the zonal schemes of Martini (1971) and Bukry (1973, 1975) but that will be employed during the Leg 108 work are also listed in Table 4.

Direct correlation to magnetostratigraphy transforms a biostratigraphic event to a biochronologic datum. A major factor influencing the precision of such correlations is the reliability of the species event used. The gathering of detailed quantitative data of biostratigraphically important species provides the only means by which the reliability of these species can be assessed. Such quantitative data exist for most of the Pliocene and Pleistocene marker species, whereas only qualitative data (presence/absence) are presently available for the Miocene and Oligocene markers. It follows that the greatest improvements regarding biochronologic precision can be expected for the older part of the sedimentary record that will be cored during Leg 108. Nevertheless, Table 4 shows the Pleistocene through latest Eocene nannofossil marker species that will be used during Leg 108 and their present-day age estimates.

In the Miocene and Oligocene, a few inconsistencies become evident when assigned age estimates of the zonal markers are

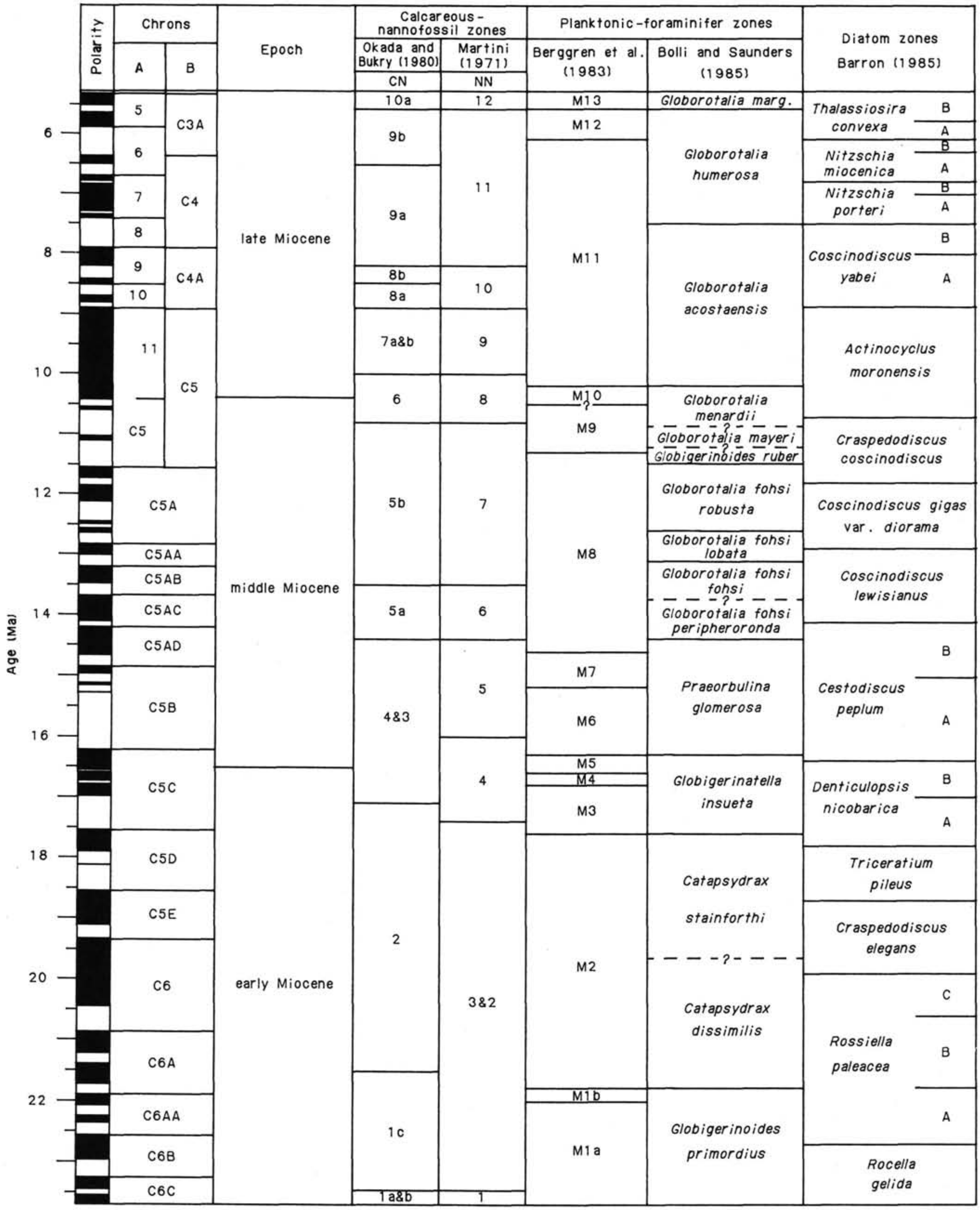

Figure 9. Miocene geochronology of Berggren et al. (1985a, 1985b) used during Leg 108.

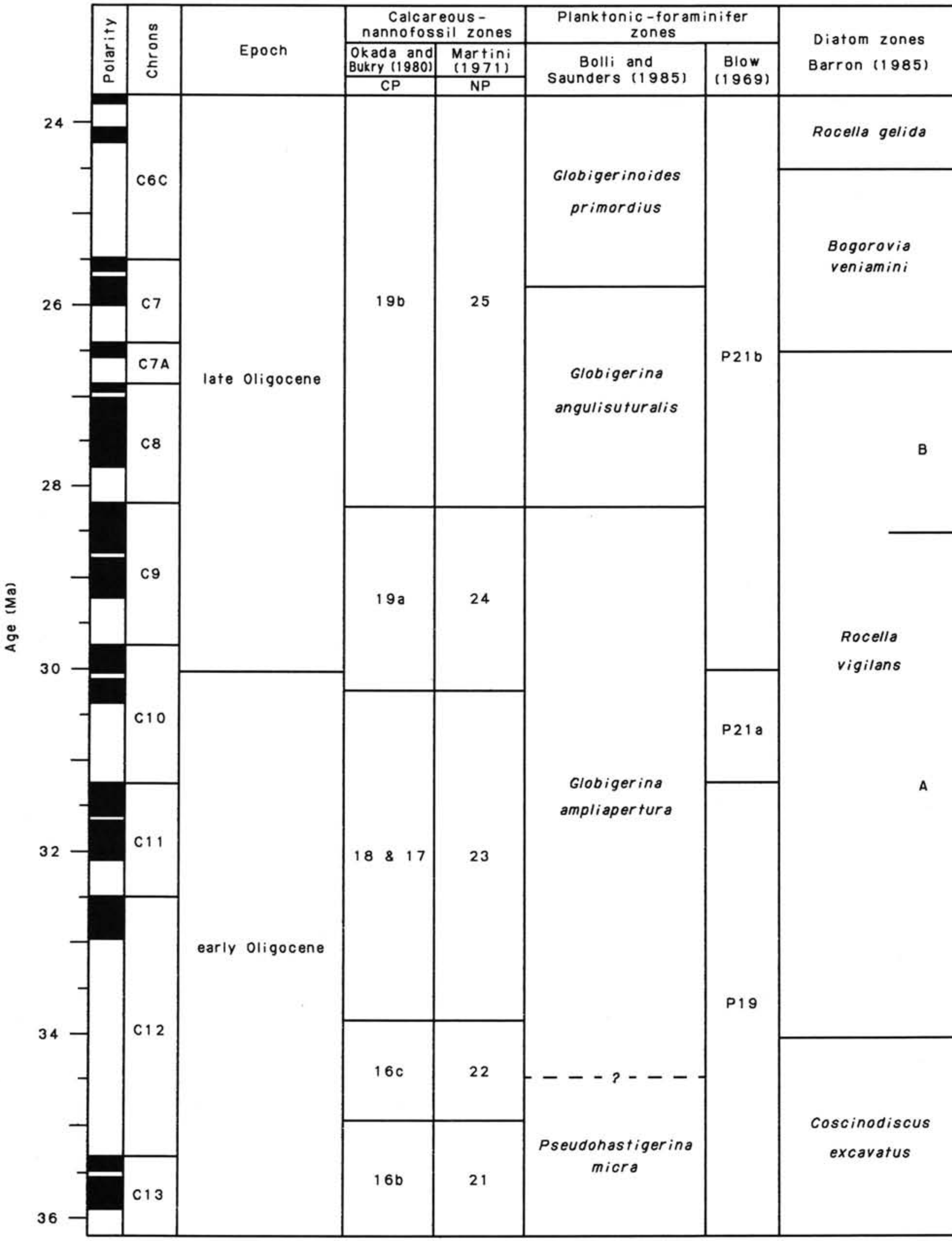

Figure 10. Oligocene geochronology of Berggren et al. (1985a, 1985c) used during Leg 108.

Table 4. Species events defining calcareous-nannofossil zonal boundaries and their assigned age estimates.

Event	Species	Zone (base)	Age (Ma)	Ref.
Increase	*Emiliania huxleyi*	—	0.085	1
FO	*E. huxleyi*	CN15/NN21	0.275	1
LO	*Pseudoemiliania lacunosa*	CN14b/NN20	0.474	1
LO	*Helicosphaera sellii*	—	1.37	2
LO	*Calcidiscus macintyrei*	—	1.45	2
FO	*Gephyrocapsa oceanica*	CN14a	1.6	3
Pliocene/Pleistocene boundary			1.66	3
FO	*Gephyrocapsa caribbeanica*	CN13b	1.7	4
LO	*Discoaster brouweri*	CN13a/NN19	1.89	2
LO	*D. triradiatus*	—	1.89	2
Increase	*D. triradiatus*	—	2.07	2
LO	*D. pentaradiatus*	CN12d/NN18	2.35	2
LO	*D. surculus*	CN12c/NN17	2.45	2
LO	*D. tamalis*	CN12b	2.65	2
LO	*Sphenolithus* spp.	CN12a	3.45	2
LO	*Reticulofenestra pseudoumbilica*	CN12a/NN16	3.56	2
Acme	*Discoaster asymmetricus*	CN11b	?	
LO	*Amaurolithus tricorniculatus*	CN11a/NN15	3.7	4
FO	*Discoaster asymmetricus*	NN14	4.1	4
LO	*Amaurolithus primus*	CN11a	4.4	4
FO	*Ceratolithus rugosus*	CN10c/NN13	4.6	2
LO	*C. acutus*	CN10c	4.6	2
FO	*C. acutus*	CN10b	5.0	4
LO	*Triquetrorhabdulus rugosus*	CN10b	5.0	4
Miocene/Pliocene boundary			5.3	4
LO	*Discoaster quinqueramus*	CN10a/NN12	5.6	4
LO	*Amaurolithus amplificus*	—	5.6	4
FO	*A. amplificus*	—	5.9	4
FO	*A. primus*	CN9b	6.5	4
FO	*Discoaster quinqueramus*	NN11	8.2	4
FO	*D. berggrenii*	CN9a	8.2	4
FO	*D. neorectus*	CN8b	8.5	4
FO	*D. loeblichii*	CN8b	8.5	4
LO	*D. hamatus*	CN8a/NN10	8.9	4
FO	*Catinaster calyculus*	CN7b	10.0	4
FO	*Discoaster hamatus*	CN7a/NN9	10.0	4
FO	*Catinaster coalitus*	CN6/NN8	10.8	4
LO	*Cyclicargolithus floridanus*	CN5b	11.6	4
FO	*Discoaster kugleri*	CN5b/NN7	13.5	4
FO	*Triquetrorhabdulus rugosus*	—	14.0	4
LO	*Sphenolithus heteromorphus*	CN5a/NN6	14.4	4
FO	*Calcidiscus macintyrei*	CN4	?	
LO	*Helicosphaera ampliaperta*	NN5	16.0	4
FO	*Sphenolithus heteromorphus*	CN3	17.1	4
LO	*S. belemnos*	NN4	17.4	4
FO	*S. belemnos*	CN2	21.5	4
LO	*Triquetrorhabdulus carinatus*	NN3	?	
FO	*Discoaster druggii*	CN1c/NN2	23.2	4
Acme	*Cyclicargolithus abisectus*	CN1b	?	
Oligocene/Miocene boundary			23.7	4
LO	*Dictyococcites bisectus*	CN1a	23.7	4
LO	*Helicosphaera recta*	NN1	?	
LO	*Sphenolithus ciperoensis*	CN1a	25.2	4
LO	*S. distentus*	CP19b/NP25	28.2	4
FO	*S. ciperoensis*	CP19a/NP24	30.2	4
FO	*S. distentus*	CP18	34.2	4
LO	*Reticulofenestra umbilicus*	CP17/NP23	33.8	5
LO	*Ericsonia obruta*	—	34.4	5
LO	*Coccolithus formosus*	CP16c/NP22	34.9	5
Increase	*Ericsonia obruta*	—	36.1	5
Eocene/Oligocene boundary			36.2	5
LO	*Discoaster saipanensis*	CP16a/NN21	36.7	5
LO	*D. barbadiensis*	CP16a	37.0	5

FO = first occurrence; LO = last occurrence. The references (right column) refer to the age column and represent (1) Thierstein et al. (1977), (2) Backman and Shackleton (1983) and Backman and Pestiaux (1987), (3) Rio et al. (in press), (4) data presented by Berggren et al. (1985a, 1985b, 1985c), (5) Backman (in press). All zonal assignments refer to the lower boundary of the zone or subzone.

compared with the stratigraphic order of the zones (Table 4). We hope that the material drilled by Leg 108 will add some insight into or resolve these problems.

Planktonic Foraminifers

Previously, the only DSDP leg to produce paleomagnetically dated tropical planktonic-foraminiferal datums was Leg 68 in the Caribbean. The data from that leg are, however, rather sparse, and the most useful sites for comparison are those from subtropical Leg 73 (Poore et al., 1984). Leg 108 should be the first leg to produce continuous Miocene to Holocene paleomagnetically dated cores from the tropical Atlantic. We therefore hope to calibrate previous zonations, such as that of Bolli and Saunders (1985), which have not been tied to paleomagnetic records, and to assess other zonations, such as the PL zonation of Berggren (1973, 1977) and the M zonation of Berggren et al. (1983), which are tied to paleomagnetic records. The Berggren zonations have been used with success at various sites, such as on the Rio Grande Rise (Berggren et al., 1983) and in the South Atlantic (Poore et al., 1984). Weaver and Clement (1986), however, found that the marker species for the PL zonation had diachronous first and last occurrences, which became progressively worse away from the subtropics in the North Atlantic. The species used by Berggren were all of warm-water preference, and thus their ranges can be expected to be more accurate in tropical areas. We will now be able to assess their usefulness in the tropical eastern Atlantic and determine whether the upwelling cells off Africa show species ranges comparable to the tropical sites or cooler water areas such as those cored on DSDP Leg 94 (Weaver and Clement, 1986).

Other tropical zonal schemes such as those of Blow (1969) and Poag and Valentine (1976) use datums that are often difficult to recognize, while those of Parker (1973), Lamb and Beard (1972), and Stainforth et al. (1975) are rather coarse, with long-ranging zones. In this work, we intend to date paleomagnetically as many foraminiferal datums as possible and to assess those most reliable for use in tropical stratigraphy. In Table 5, a list of most of the species expected to be stratigraphically useful is presented, with ages for the datums (where known) taken from Berggren et al. (1985b, 1985c).

Diatoms

Previous biostratigraphic studies of Oligocene through Quaternary diatoms for the low latitudes have concentrated on the equatorial Pacific. Significant contributions to the understanding of the Neogene diatom biostratigraphy from this region include studies by Burckle (1972, 1977, 1978), Burckle and Opdyke (1977), Burckle and Trainer (1979), Barron (1980, 1985a), Sancetta (1983), and Baldauf (1985). Oligocene and early Miocene diatom biostratigraphic studies include those by Barron (1983), Harwood (1982), and Fenner (1985).

By comparison, few studies have been completed for similar-age sediments from the low-latitude Atlantic. A preliminary examination of Miocene through Holocene diatoms recovered at DSDP Site 332 was completed by Schrader (1977). Oligocene and lower Miocene diatoms from the equatorial Atlantic region were studied recently by Fenner (1978, 1984, 1985).

The Oligocene through Holocene diatom zonation proposed by Barron (1985a, 1985b) for the equatorial Pacific was used during Leg 108 (Figs. 8 through 10). This zonation consists of 20 zones and 23 subzones. The late Miocene through Quaternary portion of Barron's zonation consists of zones originally defined by Burckle (1972, 1977). The late Oligocene through middle Miocene portion of this zonation is that of Barron (1983); the early Oligocene portion follows that of Barron (1985a) and is a modified version of the diatom zonation defined by Fenner (1985).

Table 5. Species events defining planktonic-foraminifer zonal boundaries and their assigned age estimates.

Event	Species	Zone (base)	Age (Ma)	Ref.
FO	*Globorotalia fimbriata*	*G. fimbriata*	?	5
LO	*G. tumida flexuosa*	*G. bermudezi*	?	5
FO	*Globigerina calida calida*	*G. calida*	?	5
FO	*Globorotalia crassaformis hessi*	*G. crassaformis hessi*	?	5
Pliocene/Pleistocene boundary			1.66	
FO	*Globigerinoides truncatulinoides*	*Globorotalia crassaformis viola*	1.9	5
		Globigerinoides truncatulinoides		1, 2
LO	*G. obliquus obliquus*	*G. truncatulinoides*	1.8	1, 2
LO	*Globorotalia miocenica*	*G. tosaensis*	2.2	5
		PL6		1, 2
LO	*Globigerinoides fistulosus*	*Globorotalia exilis*	?	5
LO	*Dentoglobоquadrina altispira*	PL5	2.9	1, 2
LO	*Sphaeroidinellopsis seminulina*	PL4	3.0	1, 2
LO	*Globorotalia margaritae*	PL3	3.4	1, 2
		Globigerinoides fistulosus		5
LO	*Globigerina nepenthes*	PL2	3.9	1, 2
LO	*Globoquadrina dehiscens*	PL1	5.3	1, 2
Miocene/Pliocene boundary			5.3	
FO	*Globorotalia margaritae*	*G. margaritae*	5.6	5
		M13		4
FO	*G. conomiozea*	M12	6.1	4
FO	*Neogloboquadrina humerosa*	*Globoquadrina humerosa*	7.5	5
FO	*N. acostaensis*	M11	10.2	4
		Globoquadrina acostaensis		5
FO	*Globorotalia paralenguaensis*	M10	10.5(?)	4
FO	*Globigerina nepenthes*	M9	11.3	4
LO	*Globorotalia mayeri*	*G. menardii*	?	5
LO	*Globigerinoides ruber*	*Globorotalia mayeri*	?	5
LO	*Globorotalia fohsi robusta*	*Globigerinoides ruber*	11.5	5
FO	*G. fohsi robusta*	*G. fohsi robusta*	12.6	5
FO	*G. fohsi lobata*	*G. fohsi lobata*	13.1	5
FO	*G. fohsi fohsi*	*G. fohsi fohsi*	?	5
LO	*Globigerinatella insueta*	*Globorotalia foshi peripheroronda*	14.4(?)	5
LO	*Globorotalia peripheroronda*	M8	14.6	4
FO	*Orbulina suturalis*	M7	15.2	3, 4
FO	*Praeorbulina glomerosa*	M6	16.3	3, 4
		P. glomerosa		5
FO	*P. sicana*	M5	16.6	3, 4
FO	*Globorotalia miozea*	M4	16.8	3, 4
FO	*G. zealandica*	M3	17.6	3, 4
LO	*Catapsydrax dissimilis*	*Globigerinatella insueta*	17.6	5
FO	*Globigerinatella insueta*	*Catapsydrax stainforthi*	?	5
LO	*Globorotalia kugleri*	M2	21.8	3, 4
		Catapsydrax dissimilis		5
FO	*Globoquadrina dehiscens*	M1b	22.0	3, 4
FO	*Globorotalia kugleri*	M1a	23.7	3, 4
Oligocene/Miocene boundary			23.7	
FO	*Globigerinoides primordius*	*G. primordius*	25.8	3, 4
LO	*Globorotalia opima*	*Globigerina angulisuturalis*	28.2	4
LO	*Pseudohastigerina micra*	*Globigerina ampliapertura*	?	4
LO	*Chiloguembelina*	P21b	30.0	6
FO	*Globigerina angulisuturalis*	P21a	31.2	6
FO	*G. sellii*	P19	34.0	6
Eocene/Oligocene boundary				
LO	*Hantkenina*	P18	36.6	6
LO	*Globorotalia cerroazulensis*	*Cassigerinella chipolensis*	36.6	4

FO = first occurrence; LO = last occurrence. The references (right column) refer to the age column and represent (1) Berggren (1973), (2) Berggren (1977), (3) Berggren et al. (1983), (4) Berggren et al. (1985a, 1985b, 1985c), (5) Bolli and Saunders (1985), (6) Blow (1969). All zonal assignments refer to the lower boundary of the zone or subzone.

Baldauf (1984, 1986) showed that the diatom zonation defined for the equatorial Pacific is useful with only slight modification in the middle and high latitudes of the North Atlantic. Several marker species, such as *Nitzschia miocenica, Nitzschia porteri*, and *Rhizosolenia praebergonii*, are either preservationally or ecologically excluded from the middle and high latitudes or have a sporadic occurrence and are not stratigraphically useful. Because of the geographic location of the Leg 108 sites (2°S to 21°N), it is likely that these species are present and stratigraphically useful, as they are typical of the low-latitude diatom assemblage.

Although the chronostratigraphy used during Leg 108 follows that of Berggren et al. (1985a, 1985b, 1985c), this time scale does not incorporate a diatom zonation. Therefore, direct correlations of the first (FO) or last (LO) occurrences of diatom species to a magnetostratigraphic scale follow those of Barron (1985a, 1985b). Table 6 lists the species events and their assigned age estimates. Although the majority of events have direct ties with the polarity scale, several events, primarily in the Oligocene and early Miocene, lack paleomagnetic control. In these cases, age estimates are based on extrapolation and data obtained from several DSDP or ODP sites.

Table 6. Species events defining diatom zonal boundaries and their assigned age estimates.

Event	Species	Zone (base)	Age (Ma)	Ref.
LO	*Nitzschia reinholdii*	*Pseudoeunotia doliolus*	0.65	1
LO	*Rhizosolenia matuyamai*		0.93	2
FO	*R. matuyamai*		1.00	2
LO	*R. praebergonii* var. *robustus*	B Subzone—*N. reinholdii*	1.60	3
Pliocene/Pleistocene boundary			1.66	
FO	*Pseudoeunotia doliolus*	*N. reinholdii*	1.80	3, 4, 5
LO	*R. praebergonii*		1.85	3, 5
LO	*Thalassiosira convexa* var. *convexa*	C Subzone—*R. praebergonii*	2.2	3
LO	*Nitzschia jouseae*	B Subzone—*R. praebergonii*	2.6	3
FO	*Rhizosolenia praebergonii*	*R. praebergonii*	3.0	3
LO	*Actinocyclus ellipticus* f. *lanceolata*		3.2–3.5	11
FO	*Thalassiosira convexa* var. *convexa*		3.6	5
FO	*Asteromphalus elegans*		3.9	2
LO	*Nitzschia cylindrica*		4.3	2
FO	*N. jouseae*	*N. jouseae*	4.5	2
LO	*Thalassiosira miocenica*	C Subzone—*T. convexa*	5.1	2
FO	*T. oestrupii*		5.15	12
Miocene/Pliocene boundary			5.3	
LO	*Asterolampra acutiloba*		5.35	2
LO	*Nitzschia miocenica*		5.55	2, 6
LO	*Thalassiosira praeconvexa*	B Subzone—*T. convexa*	5.8	2
FO	*T. convexa*	*T. convexa*	6.1	2
FO	*T. miocenica*		6.1	2
FO	*T. praeconvexa*	B Subzone—*N. miocenica*	6.3	2
LO	*Nitzschia porteri*		6.7	2
FO	*N. miocenica*	*N. miocenica*	6.8	2
LO	*Rossiella paleacea*		6.9	2
LO	*Thalassiosira burckliana*	B Subzone—*N. porteri*	7.0	2
FO	*Nitzschia reinholdii*		7.0	11
LO	*Coscinodiscus yabei* (= LO *C. plicatus*)	*N. porteri*	7.5	2
FO	*Thalassiosira burckliana*	B Subzone—*C. yabei*	8.0	2
LO	*Coscinodiscus temperei* var. *delicata*		8.2	13
FO	*Nitzschia fossilis*		8.2	11
LO	*Denticulopsis hustedtii* (tropical range)		8.6–8.8	11
LO	*Actinocyclus moronensis*	*C. yabei*	8.9	2
LO	*Denticulopsis punctata* f. *hustedtii*		10.7	7, 8
LO	*Craspedodiscus coscinodiscus*	*A. moronensis*	10.7	9
FO	*Hemidiscus cuneiformis*		11.2	2, 7
LO	*Actinocyclus ingens* (tropical range)		11.2–11.8	11
FO	*Coscinodiscus temperei*	*C. coscinodiscus*	11.8	8
LO	*C. lewisianus*	*C. gigas* var. *diorama*	12.9	13
FO	*Denticulopsis hustedtii* (main tropical range)		13.7	13
LO	*Cestodiscus peplum*	*C. lewisianus*	14.1	2
FO	*Coscinodiscus blysmos*		14.4	11
LO	*Annellus californicus*	B Subzone—*C. peplum*	15.0	2
LO	*Coscinodiscus praenodulifer*		15.4–15.5	11
FO	*Actinocyclus ingens* (tropical range)		15.5	13
LO	*Coscinodiscus lewisianus* var. *similis*		15.7	11
LO	*Thalassiosira fraga*		16.1–16.3	11
FO	*Cestodiscus peplum*	*C. peplum*	16.4	10
LO	*Synedra miocenica*		16.5	11
LO	*Raphidodiscus marylandicus*		16.7	11
LO	*Thalassiosira bukryi*	B Subzone—*D. nicobarica*	17.0	10
FO	*Coscinodiscus blysmos*		17.1	11
FO	*Craspedodiscus coscinodiscus* s.s.		17.3	11
FO	*Annellus californicus*		17.3	11
FO	*Coscinodiscus lewisianus* var. *similis*		17.4	11
FO	*Denticulopsis nicobarica*	*D. nicobarica*	17.8	10
LO	*Thalassiosira spinosa*		17.9	11
LO	*Actinocyclus radionovae*		18.0	10
LO	*Craspedodiscus elegans*	*T. pileus*	18.7	10
FO	*Thalassiosira fraga*		19.9	13
LO	*Bogorovia veniamini*	*C. elegans*	19.9	10
LO	*Coscinodiscus oligocenicus*	C. Subzone—*R. paleacea*	20.6	13

Table 6. (continued).

Event	Species	Zone (base)	Age (Ma)	Ref.
LO	*Melosira architecturalis*		20.6–20.9	11
FO	*Actinocyclus radionovae*		21.2	13
LO	*Thalassiosira primalabiata*	B Subzone—*R. paleacea*	21.7	13
FO	*Rossiella paleacea*	*R. paleacea*	22.7	13
Oligocene/Miocene boundary			23.7	
FO	*Rocella gelida*	*R. gelida*	24.5	11
FO	*Bogorovia veniamini*	*B. veniamini*	26.5	11
LO	*Cestodiscus mukhinae*	B Subzone—*R. vigilans*	28.5	11
LO	*Coscinodiscus excavatus*	*R. vigilans*	34.0	11
FO	*C. excavatus*	*C. excavatus*	36.5	11

FO = first occurrence; LO = last occurrence. The references (right column) refer to the age column and represent (1) Burckle (1972), (2) Burckle et al. (1978), (3) Burckle (1978), (4) Burckle (1977), (5) Burckle and Trainer (1979), (6) Barron (1985a), (7) Baldauf (1984), (8) Barron et al. (1985a), (9) Burckle et al. (1982), (10) Ciesielski (1983), (11) age extrapolated by Barron (1985a), (12) age extrapolated by Baldauf (1985), (13) age extrapolated by Barron et al. (1985a). All zonal assignments refer to the lower boundary of the zone or subzone.

Methods

Calcareous Nannofossils

Abundance. For the Leg 108 work we have chosen to define abundances of individual species as follows:

Rare: <0.1% (of the total assemblage).
Few: 0.1% to 1.0% (of the total assemblage).
Common: 1.0% to 10.0% (of the total assemblage).
Abundant: >10.0% (of the total assemblage).

Preservation. Although estimates of preservational states of the nannofossil assemblages are bound to reflect a high degree of subjectivity, some guidelines can be established. As discussed by Roth and Thierstein (1972), nannofossils are affected by both dissolution and overgrowth. These phenomena are species dependent. While some species show signs of having undergone intense dissolution, observed as broken and isolated placolith shields, enlarged central openings, etc., other species, notably the discoasters, may show overgrowth or nearly perfect preservation. Moreover, the discoasters commonly show varying degrees of overgrowth in otherwise well-preserved placolith assemblages. The discoasters range stratigraphically from the late Paleocene to the latest Pliocene, making estimates of preservational states of most Cenozoic nannofossil assemblages less meaningful if both the dissolution and overgrowth effects are not accounted for in each sample.

A simple but straightforward way to describe dissolution and overgrowth would be to characterize the dissolution effects primarily in terms of placolith preservation and overgrowth primarily in terms of discoaster preservation. It is anticipated on empirical grounds that in the sediments drilled during Leg 108 the placoliths and the discoasters will to a large extent show opposite states of preservation. Because the discoasters preferred low-latitude environments throughout their stratigraphic range, high relative abundances of discoasters will be encountered in all Leg 108 sediments older than the extinction of the last discoaster species at 1.89 Ma.

Roth and Thierstein (1972) established seven categories of preservation, one representing excellent preservation with no dissolution or overgrowth, three referring to dissolution (they used the term *etching*), and three to overgrowth. During Leg 108, we adopted Roth and Thierstein's (1972) approach for describing preservation, although a slightly modified version is used in order to adjust to ODP standards (poor, moderate, good).

G: good preservation, showing only minor or no signs of dissolution or overgrowth of placoliths and discoasters (in discoaster-bearing sediments).

Etching: E-M: slight to moderate dissolution of placoliths. In discoaster-bearing sediments and in those sediments in which both placoliths and discoasters show slight to moderate dissolution, the E-M code is used without being accompanied by an overgrowth (O) code.

E-P: severe dissolution of placoliths, abundant broken and/or isolated shields of placoliths. In discoaster-bearing sediments and in those sediments in which both placoliths and discoasters show severe dissolution, the E-P code is used without being accompanied by an overgrowth (O) code.

Overgrowth: O-M: slight to moderate overgrowth of discoasters, species still clearly recognizable. In post-discoaster-bearing sediments and in those sediments in which placoliths show slight to moderate overgrowth, the O-M code is used to signify placolith overgrowth.

O-P: severe overgrowth of discoasters, with strongly thickened arms and species often not recognizable. In post-discoaster-bearing sediments and in those sediments in which placoliths show severe overgrowth, the O-P code is used to signify severe placolith overgrowth.

Preparation. Smear-slide preparation will follow standard procedures: a small piece of sediment is smeared onto a glass slide with a drop of water, using a flat toothpick, after which a mounting medium and cover glass are applied. Samples studied in the scanning electron microscope (SEM) are dispersed in water in a test tube, either through intense shaking or by using an ultrasonic bath for about 10 to 30 s. Two to four drops of the suspension are placed on an SEM stub, dried, and coated.

Foraminifers

Samples for both planktonic and benthic foraminifers were processed by drying thoroughly and then covering with cold water. In most cases, this was sufficient to break the sample down completely; in organic-rich samples, an H_2O_2 bath was also used. The samples were then washed through a 63-μm sieve, dried under an infrared lamp, and stored. Before examination, the samples were sieved through a 150-μm sieve.

Planktonic species abundances were estimated using the following categories: rare, <3%; few, 3% to 15%; common, 15% to 30%; and abundant, >30%. No actual counts were made. Preservational characteristics were divided into three categories: good, with over 90% of the specimens unbroken; moderate, with 30% to 90% of the specimens showing dissolved or broken chambers; and poor, with samples dominated by fragments and specimens with broken or dissolved chambers.

Benthic species abundance categories are as follows: rare, <1%; few, 1% to 5%; common, 5% to 10%; and abundant, >10%. Preservation of benthic foraminifers is determined by the condition of the test and surface chambers. If, because of imperfections, <30% of the specimens examined can be identified, the preservation is considered to be poor. If between 30%

and 80% of the specimens can be identified, the preservation is considered to be moderate. If >80% of the specimens can be identified, the preservation is considered to be good.

Diatoms

Shipboard sample preparation follows the method described in Baldauf (1984), with one exception. Because of the acidity of tap water on board the *JOIDES Resolution*, decanting was generally not continued until a pH of 7 was reached. Strewn slides of acid-cleaned material were prepared on 22- by 40-mm cover glasses and mounted on 25- by 75-mm glass slides using Hyrax mounting medium.

Strewn slides were examined using a Zeiss compound microscope. At least 450 fields of view (0.5 mm diam.) were examined at 500×, with species identifications confirmed when necessary at 1250×. Species were considered *abundant* when two or more were present in one field of view at 500×, *common* if one specimen was encountered in two fields of view, *few* if one specimen was observed in one horizontal traverse, and *rare* if less than one observed per traverse. Criteria for distinguishing whole from partial diatoms follow Schrader and Gersonde (1978).

Preservation was considered *good* if more than 95% of the diatoms were whole and valves showed virtually no signs of partial dissolution, reprecipitation, or fracturing. *Moderate* preservation consisted of 30% to 95% whole valves, with moderate breakage and slight dissolution, and some fragile specimens still complete. Also, girdle bands were generally intact. If less than 30% of the diatoms were whole, preservation was regarded as *poor*. Most diatoms showed extensive breakage, partial dissolution, and pitting. Delicate structures were generally not preserved, and fragile species and girdle bands were generally not intact. If no diatoms were encountered, the sample was recorded as *barren*.

Magnetic Experiments

The magnetic experiments made in the shipboard paleomagnetic laboratory can be subdivided into three complementary parts:

1. Measurement of the natural remanent magnetization (NRM) carried out on the whole-round core sections at 5-cm intervals using the three-axis pass-through cryogenic magnetometer. This gave the values of declination, inclination, and magnetization intensity for the measured intervals.
2. Progressive demagnetization of pilot samples in alternating-current (ac) fields up to 100 mT to remove secondary components of magnetization. The pilot samples were measured with the Molspin spinner magnetometer, and the appropriate ac peak field value for blanket demagnetization could be determined from inspection of magnetization intensity and vector demagnetization plots. Samples were then demagnetized routinely at the predetermined ac peak field value and measured using a special holder placed on the core handler of the cryogenic magnetometer (eight samples were measured in one pass through the sensing region).
3. Low-field magnetic-susceptibility measurements using the Bartington whole-core sensor. Whole-core measurements were made at 3- to 20-cm intervals. The magnetic susceptibility provides an indication of downhole variations in the concentration of magnetic material.

Organic Geochemistry

During Leg 108, the following organic-geochemical measurements were performed.

Total carbon (TC), hydrogen, and nitrogen were determined using a Perkin Elmer 240C Elemental Analyzer. The method is based on combustion in pure oxygen under static conditions. The combustion products are then analyzed automatically in a self-integrating thermal-conductivity analyzer. A connected data station directly calculates weight-percentage values of carbon, hydrogen, and nitrogen.

Inorganic carbon (IC) was determined using the Coulometrics Carbon Dioxide Coulometer. The sample was treated with HCl, and the evolved CO_2 transferred to the CO_2 coulometer cell. This cell is filled with a partially aqueous medium containing ethanolamine and a coulometric indicator. When CO_2 is passed through the solution, the CO_2 is quantitatively absorbed and is converted to a strong titratable acid by the ethanolamine. The coulometer electrically generates base to return the indicator color to the starting point. Electronic scaling within the coulometer converts the number of coulombs to a digital readout of micrograms of carbon. The weight percentage of $CaCO_3$ was calculated using a conversion factor of 8.34.

The total organic carbon (TOC) was determined by difference between the total carbon (from the PE 240C Analyzer) and the inorganic carbon (from the coulometer). Comparisons of TOC data obtained by this difference method and TOC data obtained by direct measurements on acidified samples show highly similar results (shipboard reports: Eldholm, Thiede, Taylor, et al., ODP Leg 104, and Arthur, Srivastava, Clement, et al., Leg 105).

In order to characterize the type and maturity of organic matter, the Rock-Eval pyrolysis (Espitalié et al., 1977) was used. The Rock-Eval aboard *JOIDES Resolution* is a "Rock-Eval II Plus TOC" instrument that also measures the TOC content. During the analysis, the sample was heated from 250° to 550°C at a rate of 25°C/min, and the hydrocarbons thus generated were measured by a flame ionization detector (FID). CO_2, being produced by the heating and trapped until the pyrolysis temperature reaches 390°C, is measured by a thermal-conductivity detector (TCD) at the end of the analysis. In addition, the temperature of maximum pyrolysis yield (T_{max}) was determined. The amounts of generated hydrocarbons in mg HC/g TOC (hydrogen index, HI) and of CO_2 in mg CO_2/g TOC (oxygen index, OI) can give information about the type of organic matter (e.g., marine vs. terrestrial) and the hydrocarbon source potential. The T_{max} values can give information about the thermal maturity of the organic matter.

Capillary Gas Chromatography

Total soluble extracts were obtained from freeze-dried sediments by means of ultrasonic extraction with organic solvents (dichloromethane/methanol @ 2:1, 15 min, ×2). Extracts were then analyzed, without prior fractionation, using a Hewlett-Packard 5890 Gas Chromatograph operated in splitless injection mode with both inlet and detector (FID) maintained at 300°C. The column employed was a Hewlett-Packard High Performance Series OV-1 type (crosslinked methyl silicone; 25 m by 0.32 mm ID) with helium carrier gas at 25 psi head pressure. Oven temperature was controlled by multi-ramp programming, and the detector signal was monitored by a Hewlett-Packard 3392 Integrator and the Lab Automation System (LAS).

Inorganic Geochemistry

Interstitial-water samples are collected routinely and analyzed aboard ship for pH, alkalinity, salinity, calcium, magnesium, sulfate, and chlorinity. Water is squeezed from the sediments using a stainless-steel press, collected in plastic syringes, and filtered through 0.45-μm, 1-in. millipore filters.

The pH is measured using a Metrohm 605 pH-meter calibrated with 4.01, 6.86, and 7.41 buffer standards. All pH measurements are made in conjunction with alkalinity measurements. Samples are tested for pH and subsequently titrated with 0.1N

HCl, the end-point being calculated using the Gran Factor method (Gieskes and Rogers, 1973).

Salinity values are determined from refractive indices measured by an AO Scientific Instruments optical refractometer; results are given directly in ‰.

Calcium, magnesium, and sulfate concentrations are measured using the Dionex 2120i Ion Chromatograph, a dual-channel, high-performance chromatography system featuring two precision analytical pumps, a dual-channel advanced chromatography module, two conductivity detectors, an AutoIon 100 controller, and an autosampler.

Chlorinity is determined by titration with silver nitrate to a potassium chromate end-point.

Instruments are checked at each site using IAPSO standard seawater. In addition, a surface-seawater sample is collected at each site to act both as a further check of the equipment and as a test for possible drill-water contamination of interstitial-water samples.

Physical Properties

During Leg 108, physical properties were measured to determine their relationship to various sediment facies. Because of their dominant influence on seismic records, detailed physical and stratigraphic data in conjunction with digital seismic profiles will be used to decipher the origin of reflectors in seismic records by using quantitative modeling techniques (synthetic seismograms).

The on-board physical-properties program for Leg 108 includes the following measurements.

Gamma Ray Attenuation Porosity Evaluator (GRAPE)

The Gamma Ray Attenuation Porosity Evaluator (GRAPE) was used in the routine manner to log the whole-core sections. The raw data were logged on the PRO-350 and subsequently transferred to the VAX for processing. The standard procedure was used for calibration as described by Boyce (1976).

P-*Wave Logger (PWL)*

A compressional-wave whole-core logging tool (*P*-wave logger or PWL) was supplied under contract to the ODP by the Institute of Oceanographic Sciences in the United Kingdom. This device was designed to be incorporated into the new GRAPE system under development at the ODP. However, Leg 108, with its emphasis on HPC and XCB coring, provided a good opportunity to test the potential of the system prior to completion and installation of the new system. Previous detailed measurements of compressional-wave measurements (Mienert, 1985) had indicated that *P*-wave-velocity records of pelagic deep-sea sediments are applicable as a parastratigraphic tool.

The PWL is designed to log the compressional-wave velocity of whole-core sections. Typical sampling intervals would be 2 mm. The transducer frame was bolted to the GRAPE, adjacent to the source and detector such that the GRAPE and PWL could be run simultaneously. The data were logged on a BBC B microcomputer dedicated to the task. Further detailed information regarding this instrument is published elsewhere (Schultheiss, Mienert, and Shipboard Scientific Party, this volume).

Velocity

Compressional-wave-velocity measurements were also made on split cores using the Hamilton Frame Velocimeter. These measurements were taken at all the intervals where bulk density samples were taken. The operating procedure and calibration were carried out in a manner similar to that described by Boyce (1976).

Index Properties

This suite of data provided both wet and dry densities as well as other gravimetric parameters, such as water content, porosity, void ratio, and grain density. Samples of approximately 10 cm^3 were taken from freshly split cores on a routine basis of one per section down the first hole at each site, in pre-calibrated aluminum containers. Additional samples were obtained from adjacent holes to supplement the data set at intervals where the GRAPE and/or PWL indicated significant local fluctuations in density or velocity. Wet and dry weights were determined on board using the motion-compensating Scitech electronic balance to an accuracy of ± 0.02 g. Sample volumes were determined for both the wet and dry samples using the Penta Pycnometer. The samples were freeze-dried to constant weight. Samples taken for other purposes will also furnish water contents, and these data sets will be merged.

Vane Shear Strength

Because of the large amount of core material recovered on this leg, only the hand-held "Torvane" was used during the routine procedures to obtain an indication of the undrained shear strength. Previous experience (Schultheiss, 1985) had indicated that the "Torvane" provided shear-strength data comparable with that obtained with the much more time-consuming motorized vane. Some motorized-vane tests were performed on suitable samples for comparison (Boyce, 1977). It should be noted that this test is only valid in fine-grained sediments where the permeability is low enough to restrict drainage severely during the test.

Thermal Conductivity

Needle-probe measurements of thermal conductivity (Von Herzen and Maxwell, 1959) were made at selected sites.

Composite-Depth Sections

Since DSDP Leg 68, the drilling of two or more offset hydraulic-piston-corer (HPC)/advanced-piston-corer (APC) holes at a site to obtain complete recovery of the sediment sequence has become standard practice. Core breaks frequently correspond to stratigraphic discontinuities (e.g., Shackleton et al., 1984), and the presence of voids and disturbed intervals within cores can further reduce effective recovery. However, if techniques for detailed correlation are available, a sampling scheme can be devised, which, by using two or more offset holes, bypasses core breaks, other disturbed intervals, and voids.

In previous studies of DSDP HPC cores, between-hole correlation techniques have included the use of (1) sediment color changes and (2) chemical changes such as percentage of calcium carbonate variations (Leg 94; Ruddiman, Kidd, Thomas, et al., 1987). However, method 1 is subjective and at times inconclusive, and method 2 is too time consuming to be useful during the occupation of a drilling site.

During Leg 108 the problem of obtaining rapid and detailed between-hole correlations was tackled using new techniques of high-resolution (5-cm intervals or less) whole-core *P*-wave-velocity and magnetic-susceptibility logging. Details of measurement techniques, together with downhole plots of all of the *P*-wave-velocity and magnetic-susceptibility logs obtained during Leg 108, are given in Schultheiss, Mienert, and Shipboard Scientific Party (this volume) and Bloemendal, Tauxe, Valet, and Shipboard Scientific Party (this volume).

Figure 11 shows whole-core magnetic-susceptibility logs for Cores 108-665A-3H and 108-665A-4H and Core 108-665B-3H. A series of easily correlatable susceptibility features has been

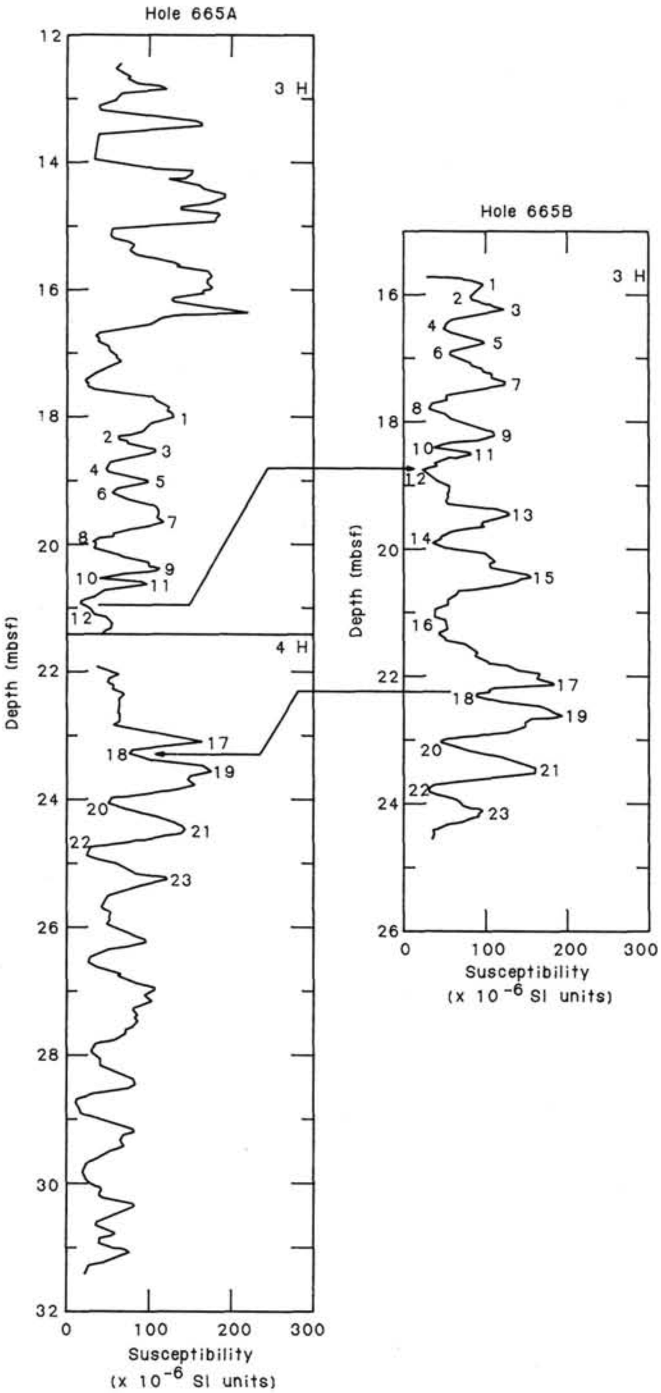

Figure 11. Whole-core magnetic-susceptibility logs for cores from Site 665, illustrating a means of circumventing the stratigraphic discontinuity across a core break. Numbers 1 through 23 indicate correlative susceptibility features.

identified and numbered from 1 to 23. Three points are relevant: (1) there is a difference of about 2 m sub-bottom depth between identical susceptibility features; (2) features 13 through 16 in Hole 665B are missing in Hole 665A, showing that a significant discontinuity occurs across the Core 108-665A 3H to 4H core break; and (3) the lack of susceptibility variation in the uppermost 1 m of Core 108-665A-4H suggests that this interval is highly disturbed.

During Leg 108, detailed comparison of whole-core susceptibility and *P*-wave-velocity logs between paired holes, together with visual inspection of the tops of split cores, showed that all of the above are common occurrences. Clearly, they constitute a significant problem for high-resolution stratigraphic studies of DSDP and ODP cores. However, if detailed correlations can be made between paired offset holes, a composite depth section can be constructed that avoids anomalous intervals such as core breaks.

Figure 11 illustrates the principle: a composite depth section for the three cores shown would begin at the top of Core 108-665A-3H, continue down to susceptibility feature 12, cross over into Core 108-665B-3H, rejoin Hole 665A at susceptibility feature 18, and continue to the base of Core 108-665A-4H. The total length of the composite section would be calculated as the sum of the within-core lengths of the three segments and at many places significantly exceeds the nominal length of sediment sections. The between-hole correlations thus provide the investigator with a "pathway" for sampling the entire correlated sequence. Correlation and sampling "pathways" are provided in each site chapter in the "Composite-Depth Section" section.

Downhole Logging

The purpose of downhole logging is the direct determination of properties of *in-situ* formations adjacent to the borehole wall. After coring is completed at a hole, a tool string is lowered downhole on a coaxial cable, with each of several tools in the tool string continuously monitoring some property of the adjacent borehole. Of the dozens of different tool strings in common use in the petroleum industry, two were selected for use on Leg 108: the Schlumberger LSS, CDIL, GR, and CAL, and the Schlumberger LDT, ZNT, and NGT.

Log Types

The physical principles and properties of the Schlumberger LSS/CDIL/MCD/GR and LDT/CNTG/NGT tools are described in previous shipboard reports and many publications (e.g., Schlumberger, 1972; Serra, 1984; Borehole Research Group, 1985) and are not repeated here in any detail.

The long-spaced sonic (LSS) has 2 transducers and 2 receivers, permitting measurements of sonic traveltime over distances of 2.4, 3.0, and 3.7 m. Two logs are recorded: the shorter spaced DR log measures the traveltime difference for the 0.6-m interval between the 2.4- and 3.0-m transducer/receiver pairs. Traveltimes are based on a simple first-break threshold criterion. Waveforms were recorded during logging upward but could not be analyzed until after the cruise.

The CDIL portion of the tool records three resistivity logs with different depths of penetration: the spherically focused log (SFL) penetrates less than 50 cm into the formation, the medium induction laterolog (ILM) penetrates about 1 to 2 m, and the deep induction laterolog (ILD) penetrates about 2 m. The resistivity logs respond primarily to formation porosity (assuming absence of hydrocarbons); some lithologic response also occurs associated with bound water in clays.

The caliper (MCD) is a three-arm (bowspring) device which measures hole diameter. It is utilized primarily for quality control and environmental correction of other types of logs.

The gamma-ray (GR) tool measures the natural gamma-ray emissions of the formation. Radioactive decay of potassium, uranium, and thorium contributes to the measured signal, but the potassium contribution is usually dominant. Traditionally considered a sand/shale indicator, the tool is more correctly described as an indicator of the relative proportion of quartz and carbonate to clay minerals, because it responds to mineralogy rather than grain size. Potassium feldspars can dominate the gamma-ray response but are usually minor in comparison to potassium-bearing clays.

The neutron tool (CNTG) uses a radioactive source to bombard the formation with neutrons. Neutrons with both "thermal" and "epithermal" energy states are captured by nuclei in the formation. Each capture is accompanied by gamma-ray emission, with an energy state dependent on the type of atom; the CNTG measures the amount of capture resulting from hydrogen. In hydrocarbon-free formations, the CNTG therefore measures total water content of the formation, including both pore spaces and bound water in clay minerals.

The natural-gamma-ray tool (NGT) is somewhat similar to the standard gamma-ray (GR) tool in that both measure natural gamma radiation emitted by formation rocks during radioactive decay of potassium, uranium, and thorium. Unlike the GR tool, which only measures total gamma rays, the NGT analyzes the spectral distribution of the gamma rays to provide accurate concentrations for the three elements. Potassium and thorium concentrations and their ratio are useful in determining the types of clay minerals present. Uranium commonly accumulates along faults or fractures; thus uranium concentration can be a fracture indicator.

The lithodensity tool (LDT) provides a measure of formation bulk density and porosity. A radioactive source mounted on a pad applied to the hole wall by an eccentering arm emits gamma rays into the formation. The gamma rays are scattered through collisions with atoms of the formation, losing energy until they are absorbed through the photoelectric effect. The number of scattered gamma rays reaching the two detectors (short and long) at fixed distances from the source is related to the electron density of the formation, which in turn depends on the true bulk density.

None of the logs discussed above is invariably reliable. All can be affected to some extent by hole conditions, such as changes in hole diameter, extensively caved intervals (washouts), and shale fracturing or alteration. The optimum logs to use in any hole may therefore depend on anticipated or experienced hole conditions as well as on scientific goals. Increasing the number of logs run causes a corresponding increase in the degree to which minor lithologic variations can be determined. Even a full suite of logs cannot compete with detailed core analysis of a single sample. Thus the primary value of logs for lithology and porosity determination lies in the fact that these variables are measured quickly and continuously over the entire logged interval. Both lithologic and porosity determination are, of course, most valuable in intervals of poor or disturbed core recovery. Porosity determination through logs has the additional virtue of measuring *in-situ* porosity prior to core disturbance by drilling or core expansion from pressure release.

Log Analysis

During logging, incoming data were observed in real time on a monitor oscilloscope and simultaneously recorded on digital tape in the Schlumberger logging unit. After logging, this tape was copied from 800 to 1600 bpi on the shipboard Vax computer system. The 1600-bpi tape was then read by the Masscomp computer system in Downhole Logging aboard ship, and reformatted to a file format compatible with the Terralog log interpretation software package. Rather than a "black box," Terralog is an interactive system consisting of a large number of log manipulation and plot options. Thus the log analysis and interpretation varied in duration and procedure for each site. Preliminary log interpretation was carried out on board; more detailed analyses are under way and will be presented in the Part B or *Final Report* portion of the Leg 108 *Proceedings* volume.

Obtaining Samples

Potential investigators wanting to obtain samples should refer to the ODP-NSF Sample Distribution Policy. Sample-request forms may be obtained from the Curator, Ocean Drilling Program, 1000 Discovery Drive, College Station, Texas 77840. Requests must be as specific as possible: include site, hole, core, section, interval within a section, and volume of sample required.

REFERENCES

Arthur, M. A., Srivastava, S., Clement, B., et al., in press. *Proc., Init. Repts. (Pt. A), ODP*, 105.

Backman, J., in press. Quantitative calcareous nannofossil biochronology of middle Eocene through early Oligocene sediment from DSDP Sites 522 and 523. *Jahrb. Oesterr. Abh.*

Backman, J., and Pestiaux, P., 1987. Pliocene *Discoaster* abundance variations, Deep Sea Drilling Project Site 606: biochronology and paleoenvironmental implications. *In* Ruddiman, W. F., Kidd, R. B., Thomas, E., et al., *Init. Repts. DSDP*, 94: Washington (U.S. Govt. Printing Office), 903–910.

Backman, J., and Shackleton, N. J., 1983. Quantitative biochronology of Pliocene and early Pleistocene calcareous nannofossils from the Atlantic, Indian and Pacific oceans. *Mar. Micropaleontol.*, 8:141–170.

Baldauf, J. G., 1984. Cenozoic diatom biostratigraphy and paleoceanography of the Rockall Plateau Region, North Atlantic, Deep Sea Drilling Project Leg 81. *In* Roberts, D., Schnitker, D., et al., *Init. Repts. DSDP*, 81: Washington (U.S. Govt. Printing Office), 439–478.

________, 1985. A high resolution late Miocene–Pliocene diatom biostratigraphy for the eastern equatorial Pacific. *In* Mayer, L., Theyer, F., et al., *Init. Repts. DSDP*, 85: Washington (U.S. Govt. Printing Office), 457–475.

________, 1986. Diatom biostratigraphic and palaeoceanographic interpretations for the middle to high latitude North Atlantic Ocean. *In* Summerhayes, C. P., and Shackleton, N. J. (Eds.), *North Atlantic Paleoceanography*: Geol. Soc. London Spec. Publ., 21:243–252.

Barron, J. A., 1980. Upper Pliocene and Quaternary diatom biostratigraphy of Deep Sea Drilling Project Leg 54, tropical eastern Pacific. *In* Rosendahl, B. R., Hekinian, R., et al., *Init. Repts. DSDP*, 54: Washington (U.S. Govt. Printing Office), 455–485.

________, 1983. Latest Oligocene through early middle Miocene diatom biostratigraphy of the eastern tropical Pacific. *Mar. Micropaleontol.*, 7:487–515.

________, 1985a. Late Eocene to Holocene diatom biostratigraphy of the equatorial Pacific Ocean, Deep Sea Drilling Project Leg 85. *In* Mayer, L., Theyer, F., et al., *Init. Repts. DSDP*, 85: Washington (U.S. Govt. Printing Office), 413–456.

________, 1985b. Miocene to Quaternary planktic diatom biostratigraphy. *In* Bolli, H. M., Saunders, J. B., and Perch-Nielsen, K. (Eds.), *Plankton Stratigraphy*: Cambridge (Cambridge Univ. Press), 763–809.

Barron, J. A., Keller, G., and Dunn, D. A., 1985a. A multiple microfossil biochronology for the Miocene. *In* Kennett, J. P. (Ed.), *The Miocene Ocean: Paleoceanography and Biogeography*: Geol. Soc. Am. Mem., 163:21–36.

Barron, J. A., Nigrini, C. A., Pujos, A., Saito, T., Theyer, F., Thomas, E., and Weinreich, N., 1985b. Synthesis of biostratigraphy, central equatorial Pacific, Deep Sea Drilling Project Leg 85: Refinement of Oligocene to Quaternary biochronology. *In* Mayer, L., Theyer, F., et al., *Init. Repts. DSDP*, 85: Washington (U.S. Govt. Printing Office), 905–934.

Berggren, W. A., 1973. The Pliocene timescale: Calibration of planktonic foraminiferal and calcareous nannoplankton zones. *Nature*, 243:391–397.

________, 1977. Late Neogene planktonic foraminiferal biostratigraphy of the Rio Grande Rise (South Atlantic). *Mar. Micropaleontol.*, 2: 251–265.

Berggren, W. A., Aubry, M. P., and Hamilton, N., 1983. Neogene magnetobiostratigraphy of Deep Sea Drilling Project Site 516 (Rio Grande Rise, South Atlantic). *In* Barker, P. F., Carlson, R. L., Johnson,

D. A., et al., *Init. Repts. DSDP*, 72: Washington (U.S. Govt. Printing Office), 675-713.
Berggren, W. A., Kent, D. V., Flynn, J. J., and Van Couvering, J. A., 1985a. Cenozoic geochronology. *Geol. Soc. Am. Bull.*, 96:1407-1418.
Berggren, W. A., Kent, D. V., and Van Couvering, J. A., 1985b. Neogene geochronology and chronostratigraphy. *In* Snelling, N. J. (Ed.), *The Chronology of the Geological Record*: Geol. Soc. London Mem., 10:211-259.
Berggren, W. A., Kent, D. V., and Flynn, J. J., 1985c. Paleogene geochronology and chronostratigraphy. *In* Snelling, N. J. (Ed.), *The Chronology of the Geological Record*: Geol. Soc. London Mem., 10:141-195.
Blow, W. H., 1969. Late middle Eocene to Recent planktonic foraminiferal biostratigraphy. *Proc. 1st Int. Conf. Planktonic Microfossils*, 1: 199-422.
Bolli, H. M., and Saunders, J. B., 1985. Oligocene to Holocene low latitude planktic foraminifera. *In* Bolli, H. M., Saunders, J. B., and Perch-Nielsen, K. (Eds.), *Plankton Stratigraphy*: Cambridge (Cambridge Univ. Press), 165-262.
Borehole Research Group, 1985. *Wireline Logging Manual*: Lamont-Doherty Geol. Observatory, for ODP.
Boyce, R. E., 1976. Appendix I. Definitions and laboratory techniques of compressional sound velocity parameters and wet-water content, wet-bulk density, and porosity parameters by gravimetric and gamma ray attenuation techniques. *In* Schlanger, S. O., Jackson, E. D., et al., *Init. Repts. DSDP*, 33: Washington (U.S. Govt. Printing Office), 931-958.
———, 1977. Deep Sea Drilling Project procedures for shear strength measurement of clayey sediment using modified Wykeham Farrance laboratory vane apparatus. *In* Barker, P. F., Dalziel, I.W.D., et al., *Init. Repts. DSDP*, 36: Washington (U.S. Govt. Printing Office), 1059-1068.
Bukry, D., 1973. Low-latitude coccolith biostratigraphic zonation. *In* Edgar, N. T., Saunders, J. B., et al., *Init. Repts. DSDP*, 15: Washington (U.S. Govt. Printing Office), 685-703.
———, 1975. Coccolith and silicoflagellate stratigraphy, northwestern Pacific Ocean, Deep Sea Drilling Project Leg 32. *In* Larson, R. L., Moberly, R., et al., *Init. Repts. DSDP*, 32: Washington (U.S. Govt. Printing Office), 677-701.
———, 1985. Mid-Atlantic Ridge coccolith and silicoflagellate biostratigraphy, Deep Sea Drilling Project Sites 558 and 563. *In* Bougault, H., Cande, S. C., et al., *Init. Repts. DSDP*, 82: Washington (U.S. Govt. Printing Office), 591-603.
Burckle, L. H., 1972. Late Cenozoic planktonic diatom zones from the eastern equatorial Pacific. *Nova Hedw.*, Beihft., 39:217-250.
———, 1977. Pliocene and Pleistocene diatom datum levels from the equatorial Pacific. *Quat. Geol.*, 7:330-340.
———, 1978. Early Miocene to Pliocene diatom datum levels for the equatorial Pacific. *Geol. Res. Dev. Cent. Spec. Publ.* (Indonesia), 1: 25-44.
Burckle, L. H., Hammond, S. R., and Seyb, S. M., 1978. A stratigraphically important new diatom from the Pleistocene of the North Pacific. *Pac. Sci.*, 32:209-214.
Burckle, L. H., Keigwin, L. D., and Opdyke, N. D., 1982. Middle and late Miocene stable isotope stratigraphy: correlation to the paleomagnetic reversal record. *Micropaleontology*, 28:329-334.
Burckle, L. H., and Opdyke, N. D., 1977. Late Neogene diatom correlations in the circum-Pacific. *Proc. 1st Init. Congr. Pac. Neogene Stratigr.*, Tokyo (Kaiyo Shuppan), 255-284.
Burckle, L. H., and Trainer, J., 1979. Middle and late Pliocene diatom datum levels from the central Pacific. *Micropaleontology*, 25:281-293.
Ciesielski, P. F., 1983. The Neogene and Quaternary diatom biostratigrahy of subantarctic sediments, Deep Sea Drilling Project Leg 71. *In* Ludwig, W. J., Krasheninnikov, V. A., et al., *Init. Repts. DSDP*, 71, Pt. 2: Washington (U.S. Govt. Printing Office), 635-665.
CLIMAP Project Members, 1981. Seasonal reconstructions of the earth's surface at the last glacial maximum. *Geol. Soc. Am. Map Chart Ser.*, M-36.
Cox, A. V., 1982. Magnetic polarity time scale. *In* Harland, W. B., Cox, A. V., Llewellyn, P. G., Smith, A. G., and Walters, R. (Eds.), *A Geologic Time Scale*: Cambridge (Cambridge Univ. Press), 63-84.
Cox, A. V., Dole, R. R., and Dalrymple, G. B., 1963. Geomagnetic polarity epochs and Pleistocene geochronometry. *Nature*, 198:1049-1051.
———, 1964. Reversals of Earth's magnetic field. *Science*, 144:1537-1543.
Dean, W. E., Leinen, M., and Stow, D.A.V., 1985. Classification of deep-sea, fine-grained sediments. *J. Sediment. Petrol.*, 55:250-256.
Eldholm, O., Thiede, J., Taylor, E., et al., in press. *Proc., Initial Repts. (Pt. A), ODP*, 104.
Emiliani, C., 1955. Pleistocene temperatures. *J. Geol.*, 63:538-578.
Espitalié, J., Madec, M., Tissot, B., Mennig, J. J., and Leplat, P., 1977. Source rock characterisation method for petroleum exploration. *Proc. 9th Annu. Offshore Technol. Conf.*, Houston, May 2-5, 439-448.
Fenner, J. 1978. Cenozoic diatom biostratigraphy of the equatorial and southern Atlantic Ocean. *In* Talwani, M., Udintsev, G., et al., *Init. Repts. DSDP*, 38, Suppl.: Washington (U.S. Govt. Printing Office), 491-624.
———, 1984. Eocene-Oligocene planktic diatom stratigraphy in the low latitudes and the high southern latitudes. *Micropaleontol.*, 30: 319-342.
———, 1985. Late Cretaceous to Oligocene planktic diatoms. *In* Bolli, H. M., Saunders, J. B., and Perch-Nielsen, K. (Eds.), *Plankton Stratigraphy*: Cambridge (Cambridge Univ. Press), 713-762.
Gartner, S., Jr., 1977. Calcareous nannofossil biostratigraphy and revised zonation of the Pliocene. *Mar. Micropaleontol.*, 2:1-25.
Gieskes, J. M., and Rogers, W. C., 1973. Alkalinity determination in interstitial waters of marine sediments. *J. Sediment. Petrol.*, 43:272-277.
Harwood, D. M., 1982. Oligocene-Miocene diatom biostratigraphy from the equatorial to the Antarctic Pacific [Master's thesis]. Florida State Univ., Tallahassee.
Hays, J. D., and Opdyke, N. D., 1967. Antarctic Radiolaria, magnetic reversals and climatic change. *Science*, 158:1001-1011.
Hedberg, H. D., Salvador, A., and Opdyke, N. D., 1979. Magnetostratigraphic polarity units—a supplementary chapter of the ISSC International Guide. *Geology*, 7:578-583.
LaBrecque, J. L., Hsü, K. J., Carman, M. F., Jr., Karpoff, A. M., McKenzie, J. A., Percival, S. F., Jr., Petersen, N. P., Pisciotto, K. A., Schreiber, E., Tauxe, L., Tucker, P., Weissert, H. J., and Wright R., 1983. DSDP Leg 73: Contributions to Paleogene stratigraphy in nomenclature, chronology and sedimentation rates. *Palaeogeogr., Palaeoclimatol., Palaeoecol.*, 42:91-125.
Lamb, J. L., and Beard, J. H., 1972. Late Neogene planktonic foraminifers in the Caribbean, Gulf of Mexico, and Italian stratotypes. *Univ. Kansas Paleontol. Contrib.*, 57.
Martini, E., 1971. Standard Tertiary and Quaternary calcareous nannoplankton zonation. *In* Farinacci, A. (Ed.), *Proc. II Plankt. Conf., Roma, 1971*: Rome (Ed. Tecnoscienza), 739-777.
Matthews, D. J., 1939. *Tables of Velocity of Sound in Pore Water and in Seawater*: London (Admiralty, Hydrogr. Dep.).
Mienert, J., 1985. Physikalische Sedimenteigenschaften: P-Wellengeschwindigkeiten. *In* Sarnthein, M., Haake, F., Mayer, L., Pflaumann, U., Springer, M., Werner, P., and Wiederhold, H., Report of R.V. "Polarstern" cruise Ant IV/1c to the equatorial Atlantic GEOTROPEX '85 Dakar-Rio de Janeiro, October 14-November 3. *Rep., Geol. Paläontol. Inst. Univ. Kiel*, 11:35.
Miller, K. G., Aubus, M. P., Khan, M. J., Mebillo, A. J., Kent, D. V., and Berggren, W. A., 1985. Oligocene-Miocene biostratigraphy, magnetostratigraphy and isotope stratigraphy of the western North Atlantic. *Geology*, 13:257-261.
Munsell Soil Color Charts, 1971. Baltimore (Munsell Color).
Okada, H., and Bukry, D., 1980. Supplementary modification and introduction of code numbers to the low-latitude coccolith biostratigraphic zonation (Bukry, 1973, 1975). *Mar. Micropaleontol.*, 5:321-325.
Parker, F. L., 1973. Late Cenozoic biostratigraphy (planktonic foraminifera) of tropical deep-sea sections. *Rev. Esp. Micropaleontol.*, 5: 253-289.
Poag, C. W., and Valentine, P. C., 1976. Biostratigraphy and ecostratigraphy of the Pleistocene basin, Texas-Louisiana continental shelf. *Trans. Gulf Coast Assoc. Geol. Soc.*, 26:185-256.
Poore, R. Z., Tauxe, L., Percival, S. F., Jr., LaBrecque, J. L., Wright, R., Petersen, N. P., Smith, C. C., Tucker, P., and Hsü, K. J., 1984.

Late Cretaceous–Cenozoic magnetostratigraphic and biostratigraphic correlations for the South Atlantic Ocean, Deep Sea Drilling Project Leg 73. *In* Hsü, K. J., LaBrecque, J. L., et al., *Init. Repts. DSDP*, 73: Washington (U.S. Govt. Printing Office), 645–655.

Rio, D., Backman, J., and Raffi, I., in press. *Calcareous Nannofossil Biochronology and the Pliocene/Pleistocene Boundary*: Micropaleontol. Press Spec. Publ.

Roth, P. H., and Thierstein, H., 1972. Calcareous nannoplankton: Leg 14 of the Deep Sea Drilling Project. *In* Hayes, D. E., Pimm, A. C., et al., *Init. Repts. DSDP*, 14: Washington (U.S. Govt. Printing Office), 421–485.

Ruddiman, W. F., Kidd, R., Thomas, E., et al., 1987. *Init. Repts. DSDP*, 94: Washington (U.S. Govt. Printing Office).

Ryan, W.B.F., Cita, M. B., Rawson, M. D., Burckle, L. H., and Saito, T., 1974. A paleomagnetic assignment of Neogene stage boundaries and the development of isochronous datum planes between the Mediterranean, the Pacific and Indian oceans in order to investigate the response of the world ocean to the Mediterranean "Salinity Crisis." *Riv. Ital. Paleontol.*, 80:631–688.

Sancetta, C. A., 1983. Biostratigraphic and paleoceanographic events in the eastern equatorial Pacific: results of Deep Sea Drilling Project Leg 69. *In* Cann, J. R., Langseth, M. G., Honnorez, J., Von Herzen, R. P., White, S. M., et al., *Init. Repts. DSDP*, 69: Washington (U.S. Govt. Printing Office), 311–320.

Sarnthein, M., Thiede, J., Pflaumann, U., Erlenkeuser, H., Fütterer, D., Koopmann, B., Lange, H., and Seibold, E., 1982. Atmospheric and oceanic circulation patterns off Northwest Africa during the past 25 million years. *In* von Rad, U., Hinz, K., Sarnthein, M., and Seibold, E. (Eds)., *Geology of the Northwest African Continental Margin*: Berlin-Heidelberg (Springer-Verlag), 545–604.

Schlumberger, Inc., 1972. *The Essentials of Log Interpretation Practice*.

Schrader, H.-J., 1977. Diatom biostratigraphy, Deep Sea Drilling Project Leg 37. *In* Aumento, F., Melson, W. G., et al., *Init. Repts. DSDP*, 37: Washington (U.S. Govt. Printing Office), 967–975.

Schrader, H.-J., and Gersonde, R., 1978. Diatoms and silicoflagellates. *Utrecht Micropaleontol.*, 17:129–176.

Schultheiss, P. J., 1985. Physical and geotechnical properties of sediments from the Northwest Pacific: Deep Sea Drilling Project Leg 86. *In* Heath, G. R., Burckle, L. H., et al., *Init. Repts. DSDP*, 86: Washington (U.S. Govt. Printing Office), 701–722.

Serra, O., 1984. *Fundamentals of Well Log Interpretation*: Amsterdam (Elsevier).

Shackleton, N. J., Backman, J., Zimmerman, H., Kent, D. V., Hall, M. A., Roberts, D. G., Schnitker, D., Baldauf, J. G., Desprairies, A., Homrighausen, R., Huddlestun, P., Keene, J. B., Kaltenback, A. J., Krumsiek, K.A.O., Morton, A. C., Murray, J. W., and Westburg-Smith, J., 1984. Oxygen isotope calibration of the onset of ice-rafting and history of glaciation in the North Atlantic region. *Nature*, 307:620–623.

Stainforth, R. M., Lamb, J. L., Luterbacher, H., Beard, J. H., and Jeffords, R. M., 1975. *Cenozoic Planktonic Foraminiferal Zonation and Characteristics of Index Forms*: Univ. Kansas Paleontol. Contrib., Art. 62.

Tauxe, L., Monaghan, M., Drake, R., Curtis, G., and Staudigel, H., 1985. Paleomagnetism of Miocene east African rift sediments and the calibration of the geomagnetic reversal time scale. *J. Geophys. Res.*, 90:4639–4646.

Thierstein, H. R., Geitzenauer, K. R., Molfino, B., and Shackleton, N. J., 1977. Global synchroneity of late Quaternary coccolith datum levels: validation by oxygen isotopes. *Geology*, 5:400–404.

Vine, F., and Matthews, D. H., 1963. Magnetic anomalies over ocean ridges. *Nature*, 199:947–949.

Von Herzen, R. P., and Maxwell, A. E., 1959. The measurements of thermal conductivity of deep-sea sediments by a needle probe method. *J. Geophys. Res.*, 64:1557–1563.

von Rad, U., Hinz, K., Sarnthein, M., and Seibold, E. (Eds.), 1982. *Geology of the Northwest African Continental Margin*: Berlin-Heidelberg (Springer-Verlag).

Weaver, P.P.E., and Clement, B. M., 1986. Synchroneity of Pliocene planktonic foraminiferal datums in the North Atlantic. *Mar. Micropaleontol.*, 10:295–307.

Wentworth, C. K., 1922. A scale of grade and class terms of clastic sediments. *J. Geol.*, 30:377–390.